M 2023

U.PORTO
FEUP FACULDADE DE ENGENHARIA
UNIVERSIDADE DO PORTO

Study of the technical and economic viability of an innovative process for the capture of biogenic CO_2

JOSÉ FRANCISCO FONTES MARQUES
MASTER THESIS IN CHEMICAL ENGINEERING
PRESENTED TO THE FACULTY OF ENGINEERING
OF THE UNIVERSITY OF PORTO

Master in Chemical Engineering

Study of the technical and economic viability of an innovative process for the capture of biogenic CO_2

Master dissertation

of

José Francisco Fontes Marques

Developed within the course of dissertation

held in

CapWatt and Carbopora

Supervisor at FEUP: **Doctor Tânia Lopes**

Joint supervisor(s) at FEUP: **Professor Adélio Mendes**

Coordinator at Capwatt: **Engineer Pedro Vieira**

Coordinator at Carbopora: **Manuel Lopes**

July 2023

Acknowledgment

A special thank you to my supervisor, Dr. Tânia Lopes, for the countless hours spent helping me develop this master thesis, for the endless meetings, and above all for the invaluable guidance provided that enabled me to confront this challenge with the mindset of a true engineer.

To Professor Adélio Mendes, thank you for the immense inspiration and the curiosity for constant knowledge. Thank you for the exceptional mentoring and for always encouraging me to strive for excellence.

A special thank you to Professor Fernando Martins for every word of encouragement and the help given with the Aspen Plus software. This helped enable the quality of the results here presented.

To Eng. Pedro Vieira, thank you for receiving me and for the opportunity to apply my knowledge to the business world. Without your help, this work wouldn't have been possible.

To my parents, sisters, and close family, a big thank you for all the values and strength you all have instilled in me, always encouraging me to give my best even when times are difficult.

To all my friends, thank you for giving me the best university experience one could have asked. Your presence made every difficult moment so much easier. To Inês, thank you for being with me every step of the way with this master thesis. To Sofia and Matilde, you know I don't have words that can describe what the two of you mean to me. To Miguel, you know what I am not able to put into words.

Lastly, to Tiago Araújo and Telmo Lopes, thank you for helping me in every step of the way. For clarifying all my doubts and going out of your way to ensure that this thesis is something I can be proud of.

Professor Adélio Mendes and Dr Tânia Lopes, supervisors of this dissertation are integrated members of LEPABE – Laboratory for Process Engineering, Environment, Biotechnology and Energy, financially supported by LA/P/0045/2020 (ALiCE), UIDB/00511/2020 and UIDP/00511/2020 (LEPABE), funded by national funds through FCT/MCTES (PIDDAC).

Abstract

Carbon capture and storage (CCS) technologies are expected to play a vital role in upholding the global climate goals. These are often referred to as promising countermeasures to mitigate CO_2 emissions from energy-intensive sectors. Within the scope of this thesis, these technologies will be applied to Capwatt's biomass plant in Mangualde, that emits 90000 $Nm^3 \cdot h^{-1}$ of flue gas, of which 14.5 % is CO_2. Belonging to the Sonae universe, Capwatt is a Portuguese company committed to developing energy measures to ensure sustainable solutions. This thesis aims to determine the most cost-effective CCS technology to capture and purify CO_2 to the input requirements for methanol synthesis, while integrating Carbopora's membrane technology as a possible solution for the separation process. Aspen Plus software and a newly developed Python code are used in the design and optimization of the processes. The focus, through selection, is to assess the feasibility of membrane separation, both polymeric and inorganic, as well as CO_2-Monoethanolamine (MEA) for CCS, based on their overall cost-effectiveness. It is determined that MEA-based absorption, although effective, is more expensive and energy-consuming compared to membrane separation. However, the latter require large membrane area to achieve higher recovery rates. The relationship between membrane area and specific cost was determined, and the best compromise between both was identified. Additionally, the influence of the feed pressure on the recovery and purity values was evaluated. For polymeric membranes, three membrane stages without recycling and 1.5 bar feed pressure were identified as the optimal solution, with an estimated cost of 40.70 $€ \cdot tonCO_2^{-1}$ to separate the CO_2 gas. With inorganic membranes, the results indicate that, for the same process configuration, a feed pressure of 6 bar provides the lowest specific cost for a total process cost of 118.80 $€ \cdot tonCO_2^{-1}$.

To increase the purity of the CO_2 gas stream and reach the required pressure of 70 bar for the direct hydrogenation process of CO_2 to green methanol, an additional purification step is considered. To achieve the desired purity levels of 99.9 %, and a CO_2 recovery greater than 80 %, it has been determined that the overall costs for separation and purification are 111.40 $€ \cdot tonCO_2^{-1}$, 93.24 $€ \cdot tonCO_2^{-1}$ and 221.50 $€ \cdot tonCO_2^{-1}$ for MEA absorption, polymeric and inorganic membrane technologies, respectively. This study demonstrates that membrane separation, particularly polymeric, is the most cost-effective and energy-efficient technology for CCS. Additionally, it provides development guidance to Carbopora to make its inorganic membranes a more competitive solution for CCS.

Keywords: Membranes, Separation, Purification, Absorption, CO_2 capture

Resumo

É expectável que as tecnologias de captura e armazenamento de carbono (CCS) desempenhem um papel vital no cumprimento das metas climáticas globais. Muitas vezes referido como uma medida promissora para mitigar as emissões de CO_2 do setor da energia e outros de uso intensivo da mesma. No âmbito desta tese, estas tecnologias serão aplicadas à central de biomassa da Capwatt em Mangualde, que emite 90000 $Nm^3 \cdot h^{-1}$ de gases de combustão, dos quais 14,5 % é CO_2. Pertencente ao universo Sonae, a Capwatt é uma empresa portuguesa que procura desenvolver soluções sustentáveis. Esta tese visa determinar a tecnologia CCS mais rentável para capturar e purificar CO_2 até ás condições necessárias para a síntese de metanol, integrando simultaneamente a tecnologia de membranas da Carbopora como uma possível solução para o processo de separação. O software Aspen Plus e um simulador desenvolvido na linguagem de Python foram usados no projeto e respetiva otimização dos processos. O foco, por meio de seleção, é avaliar a viabilidade da separação por membranas, tanto poliméricas quanto inorgânicas, bem como CO_2-monoetanolamina (MEA) para CCS, com base no seu custo-benefício. É determinado que a absorção baseada em MEA, embora eficaz, é mais cara e consome mais energia em comparação com a separação por membranas. No entanto, e para atingir taxas de recuperação mais elevadas, estas últimas, necessitam de elevadas áreas de membrana. A relação entre área da membrana e o custo específico foi determinado, e identificou-se qual o melhor compromisso entre ambos. Adicionalmente, foi avaliada a influência da pressão de alimentação nos valores de recuperação e pureza. Para membranas poliméricas, três estágios de membrana sem reciclagem e pressão de alimentação de 1,5 bar são identificados como a solução ideal, com um custo estimado de 40,70 €$\cdot ton CO_2^{-1}$ para separar o gás CO_2. Com membranas inorgânicas, os resultados indicam que, para a mesma configuração de processo, uma pressão de alimentação de 6 bar proporciona o menor custo específico com um custo total de 118,80€$\cdot ton CO_2^{-1}$. Para aumentar a pureza do fluxo de gás CO_2 e atingir a pressão necessária de 70 bar para o processo de hidrogenação direta de CO_2 para metanol verde, é considerada uma etapa adicional de purificação. Para se atingir os níveis de pureza desejados de 99,9 %, e uma recuperação de CO_2 superior a 80 %, determinou-se que os custos gerais para separação e purificação são 111,40 €$\cdot ton CO_2^{-1}$, 93,24 €$\cdot ton CO_2^{-1}$ e 221,50 €$\cdot ton CO_2^{-1}$ para absorção de MEA, tecnologias de membrana polimérica e inorgânica, respetivamente. Este estudo demonstra que a separação por membrana, particularmente poliméricas é a tecnologia económica e energeticamente mais eficiente para CCS. Adicionalmente, fornece orientações de desenvolvimento à Carbopora para tornar as suas membranas inorgânicas uma solução mais competitiva para CCS.

Palavras Chaves: Membranas, Separação; Purificação; Absorção, Captura de CO_2

Declaration

I hereby declare, under word of honour, that this work is original and that all non-original contributions is indicated and due reference is given to the author and source

Sign and date

José Francisco Fontes Marques

03/07/2023

Index

1. Introduction 1

1.1 Motivation 1

1.2 Presentation of the company 2

1.3 Organization of the dissertation 3

2. Context and State of the art 4

2.1 Carbon Capture and Storage 4

2.1.1 Pre-combustion 5

2.1.2 Oxyfuel 5

2.1.3 Post-Combustion 6

2.2 Separation Process 7

2.2.1 Separation by Absorption 7

2.2.2 Separation by Adsorption 10

2.2.3 Cryogenic Distillation 10

2.2.4 Membrane Separation 11

2.3 Purification Process 13

2.3.1 Purification by Compression 14

2.3.2 Purification by Liquefaction 14

3. Materials and Methods 15

3.1 CO_2 Capture Process – Case Study 15

3.2 Development of the gas permeation model 17

3.3 Simulation with Aspen Plus 18

3.4 Cost model and equipment sizing 19

4. Results and Discussion 22

4.1 CO_2 Separation by Absorption with MEA solvent 22

4.2 CO_2 Separation with Membrane Technology 25

4.2.1 Model validation 25

4.2.2 Polymeric Membranes 26

4.2.3 Inorganic Membranes 33

4.3 Purification Process 38

4.3.1 Purification Process post Separation by Absorption 38

4.3.2 Purification Process post Separation by Membrane Technology 39

4.4 Technology Comparison 41

4.5 Sensitivity Analysis 43

4.5.1 Influence of Electricity Cost 43

4.5.2 Influence of Inorganic Membrane Cost 43

4.5.3 Influence of Inorganic Membrane Permeances 44

5. Conclusion 45

6. Assessment of the work done 46

6.1 Future Work 46

6.2 Other Work Carried Out 46

6.3 Final Assessment 46

7. References 47

Annex A – Additional information regarding equipment cost estimation 51

Appendix A – Additional information regarding Separation by Adsorption 52

Appendix B - Separation Processes Comparison 53

Appendix C – Additional configurations for Membrane Separation 54

Appendix D – Equipment sizing for the Separation Process with Absorption 56

Appendix E – Equipment sizing for the Separation Process with Membrane Technology .. 57

Appendix F – Equipment sizing for the Purification Process post Absorption 58

Appendix G – Equipment sizing for the Purification Process post Membrane Separation .. 59

List of Figures

Figure 1. *(A) Global greenhouse emissions by gas and (B) Plot of global CO_2 emissions over time (Reproduced from [2]).* *1*

Figure 2. *CO_2 phase diagram (Reproduced from [7]).* *4*

Figure 3. *Representation of the different separation processes for CCS.* *7*

Figure 4. *Schematic diagram of a CO_2 absorption plant (Reproduced from [12])*..... *8*

Figure 5. *Scheme of a membrane separation (Reproduced from [21]).* *11*

Figure 6. *Schematic representation of CO_2 purification process through Compression/liquefaction (Reproduced from [28]).* *13*

Figure 7. *Schematic representation of Cryocap™ FG for purification of CO_2 (Reproduced from [29]).* . *14*

Figure 8. *Schematic presentation of the different pathways for a carbon Capture Process.* *15*

Figure 9. *Illustrative ideal membrane separation process configuration with the respective mass balance at an infinitesimal area.* *17*

Figure 10. *Schematic of the separation process through absorption using MEA as solvent.* *23*

Figure 11. *A) Cost distribution for the simulated absorption process, and B) distribution of the energy spending for the process.* *25*

Figure 12. *Schematic representation of the best configuration for the separation process using membrane technology.* *28*

Figure 13. *A) Relation between recovery and accumulated membrane area, and B) Relation between purity and accumulated membrane area for various feed pressures with 3 polymeric membrane stages.* *28*

Figure 14. *A) Relation between recovery and accumulated membrane area, and B) Relation between purity and accumulated membrane area for various feed pressures with 3 polymeric membrane stages.* *29*

Figure 15. *Recovery and Purity trade-off plot.* *30*

Figure 16. *Relation between feed pressure, recovery, and accumulated membrane area for a fixed purity of 97.5%.* *30*

Figure 17. *Schematic representation of the best configuration for the separation process using polymeric membrane technology.* *31*

Figure 18. *Cost distribution for the polymeric membrane technology process.* *32*

Figure 19. *A) Relation between recovery and accumulated membrane area, and B) Relation between purity and accumulated membrane area for various feed pressures with 3 inorganic membrane stages.* *34*

***Figure 20**. A) Relation between purity and specific cost, and B) Relation between purity and specific cost for various feed pressures with 3 inorganic membrane stages. 35*

***Figure 21**. Recovery and Purity trade-off plot. 35*

***Figure 22**. Schematic representation of the best configuration for the separation process using inorganic membrane technology. 36*

***Figure 23**. Cost distribution for the simulated inorganic membrane technology process. 37*

***Figure 24**. Schematic representation for the purification process after separation with Absorption. . 38*

***Figure 25**. Schematic representation of the designed purification process for both membrane technologies – polymeric and inorganic. 40*

***Figure 26**. Feed pressure influence on the specific cost and power demand for Separation + Purification process with: A) polymeric membranes and B) inorganic membranes. 40*

***Figure 27**. Entire cost distribution for all three simulated Separation processes. 42*

***Figure 28**. Cost distribution for the simulated Separation+Purification processes. 42*

***Figure 29**. Influence of Electricity cost on overall cost for Separation+Purification for both polymeric and inorganic membranes. 43*

***Figure 30**. Influence of membrane cost on specific cost of Separation+Purification for inorganic membrane technology. 44*

***Figure 31**. Influence of the CO_2 permeance on overall specific cost of Separation+Purification for inorganic membrane technology compared with the optimal cost for polymeric membrane technology. 44*

***Figure 32**. Pump purchase cost according to its capacity (Reproduced from [35]). 51*

***Figure 33**. Schematic representation of configuration B for the Separation Process using Membrane Technology. 54*

***Figure 34**. Schematic representation of configuration C for the Separation Process using Membrane Technology. 54*

***Figure 35**. Schematic representation of configuration D for the Separation Process using Membrane Technology. 55*

List of Tables

Table 1. *Advantages and Disadvantages of the studied separation processes.* *16*

Table 2. *Parameters used to determine EAC with Equation 3.24.* *21*

Table 3. *Definition and value for the parameters needed for OPEX calculations.* *21*

Table 4. *Flow rate composition for flue gas post pre-treatment*..... *22*

Table 5. *Results obtained from the separation process through absorption with MEA solvent*..... *24*

Table 6. *Overall expenditure results concerning absorption process with MEA solvent.* *24*

Table 7. *Comparison of simulation models.* *26*

Table 8. *Polymeric membrane performance parameters (Reproduced from [42]).* *26*

Table 9. *Stage number influence on overall membrane separation performance*..... *27*

Table 10. *Configuration influence on overall membrane separation.*..... *27*

Table 11. *Operational conditions and respective separation results from a membrane separation process according to configuration A, with vacuum pressure at permeate side for all stages.* *31*

Table 12. *Overall expenditure results from a separation process with polymeric membrane technology.* *32*

Table 13. *Inorganic membrane performance parameters.*..... *33*

Table 14. *Stage number influence on overall membrane separation performance.* *33*

Table 15. *Configuration influence on overall membrane separation.*..... *34*

Table 16. *Operation conditions and results from inorganic membrane separation according to configuration A, with vacuum pressure at permeate side for all stages*..... *36*

Table 17. *Overall expenditure results for a separation process with inorganic membranes.*..... *37*

Table 18. *Overall expenditure results for Separation+Purification process post Absorption separation.* *38*

Table 19. *Overall expenditure results concerning this Separation+Purification processes through both membrane technologies for a feed pressure of the optimised values of 1.5 and 6 bar.*..... *41*

Table 20. *Comparison of Performance and Cost Metrics for Simulated CCS Processes in Separation and Purification Stages combined.* *41*

Table 21. *Decision factor for the main technologies for the separation process in CCS.*..... *53*

Table 22. *Pumps characteristics for the Absorption Process.* *56*

Table 23. *Heat exchanger characteristics for the Absorption Process.* *56*

Table 24. *Absorber and Stripper columns characteristics for the Absorption Process.* *56*

Table 25. *Compressing equipment characteristics for Purification Process post Membrane Separation.* *57*

Table 26. *Compressing equipment characteristics for Purification Process post Absorption.* *58*

Table 27. *Heat exchanger characteristics for Purification process post Absorption Process.*..... *58*

Table 28. *Flash separators' characteristics for Purification Process post Absorption Process.*..... *58*

Table 29. *Compressing equipment characteristics for Purification Process post both Membrane Technologies Processes.* *59*

Table 30. *Heat exchangers characteristics for Purification Process post both Membrane Technologies Processes.* *60*

Table 31. *Flash separators' characteristics for Purification process post both Membrane Technologies Processes.* *60*

Notation and Glossary

A	Area	m^2
A_T	Total membrane area	m^2
$C_{compressor}$	Cost of compressor	€
$C_{cooling\ water}$	Cooling Water rate cost	€·m^{-3}
C_{CW}	Cost of Cooling Water	€
C_E	Cost of Electricity	€
$C_{Electricity}$	Electricity rate cost	€·kwh^{-1}
$C_{Equipment}$	Total cost of the added equipment	€
C_h	Cost of Heat exchanger	€
C_{HO}	Cost of Hot oil	€
$C_{Hot\ Oil}$	Hot oil rate cost	€·m^{-3}
$C_{membrane}$	Membrane cost	€
C_{PL}	Additional cost of platforms and stairs	€
C_{RL}	Cost of Refrigerant liquid	€
$C_{Ref.\ Liquid}$	Refrigerant liquid rate cost	€·GJ^{-1}
$C_{Separator}$	Cost of Flash separator	€
C_S	Cost of steam	€
C_{Steam}	Steam rate cost	€·$MMBTU^{-1}$
C_v	Cost of empty equipment	€
$C_{vacuum\ pump}$	Cost of vacuum pump	€
D_i	Internal diameter of equipment	m
F_F	Membrane feed flow	mol·m^{-1}
F_M	Material factor	
F_P	permeate flow rate at the membrane outlet	mol·m^{-1}
F_R	Retentate flow rate at the membrane outlet	mol·m^{-1}
h	Column height	m
I	Product cost Index	
J_i	Flux rate of component *i* across the membrane	mol·m^{-2}·s^{-1}
K_M	Membrane unit cost	€·m^{-2}
L	Membrane length	m
$\mathcal{L}_i$	Permeance of component i	mol·m^{-2}·Pa^{-1}·s^{-1}
P_C	Power duty for compressors and pumps	kW
P_{ent}	Inlet pressure to the membrane	bar
P_F	Membrane Feed pressure	bar
P_P	Permeate stream pressure	bar
P_R	Retentate stream pressure	bar
P_1	Power for hot oil utility	kcal·hr^{-1}
P_2	Volumetric flow rate for cooling water utility	m^3·hr^{-1}
P_3	Energy flow rate for refrigerant liquid utility	GJ·hr^{-1}
P_4	Energy flow rate for steam utility	MMBTU·hr^{-1}
Q	Gas flow for compression	mol s^{-1}
r	Membrane radius	m
R	Ideal gas constant	J·K^{-1}·mol^{-1}
T	Temperature	ºC
t_{op}	Annual operating time	h·$year^{-1}$
t	Membrane thickness	m
VLH	Volumetric lower heating value	kcal·m^{-3} PTN
$x_{i,F}$	Mole fraction of component *i* in the feed stream	
$x_{i,R}$	Mole fraction of component *i* in the retentate stream	
W	Column Weight	kg
$y_{i,P}$	Mole fraction of component *i* in the permeate stream	

z	Dimensionless coordinate	

Greek Letters

γ	Coefficient of gas expansion	
η_C	Compressor isentropic efficiency	
ρ	Fluid density	$kg \cdot m^{-3}$

Indexes

i	Component *i* (CO_2, N_2, O_2)	

List of Acronyms

CAPEX	*Capital Expenditure*
CCS	Carbon Capture and Storage
CEPSI	*Chemical Engineering Plant Cost Index*
EAC	Estimated Annual Cost
IL	Ionic Liquids
MEA	Monoethanolamine
MOF	Meta-organic framework
OPEX	*Operational Expenditure*
PSA	Pressure Swing Adsorption
TSA	Temperature Swing Adsorption
VSA	Vacuum Swing Adsorption

1. Introduction

1.1 Motivation

The urgency of the current climate emergency motivated the Paris Agreement, an accord signed by 196 countries and the European Union in 2015. It put forward an unprecedented plan to confront the consequences of this crisis head-on and pledged to limit the rise of the globe's temperature to a maximum of 2.0 °C by 2050. Such is only feasible by targeting the main sources of this issue. Over the last few decades, greenhouse gas emissions have been linked to the observed environmental issues, climate change, and global warming. Around 97 % of active climate scientists believe that human activity is causing these greenhouse emissions and, therefore, this environmental crisis. Carbon dioxide (CO_2) is the greenhouse gas most emitted to the atmosphere, accounting for approximately 76% of total emissions (**Figure 1**). Given its significant contribution, the Paris agreement surged the initiatives to curtail carbon emissions dramatically [1].

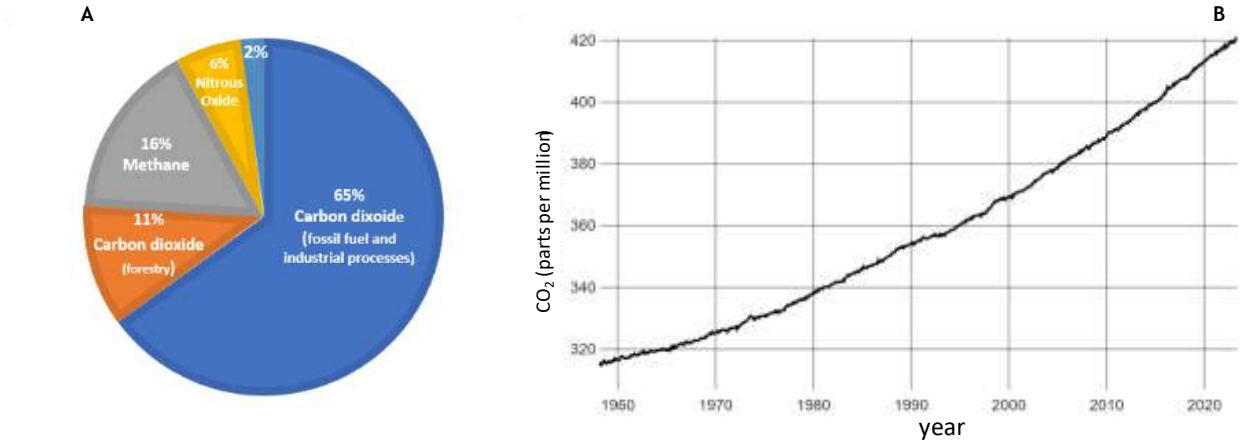

Figure 1. (A) Global greenhouse emissions by gas *and* (B) Plot of global CO_2 emissions over time (Reproduced from [2]).

The data in **Figure 1** exhibits a contrary trend to the objective set forth in the Paris Agreement, as carbon emissions remain predominant and have continuously increased for the past decades. This continuous and sharp rise in CO_2 fraction of emissions is due to an increase in energy consumption from the burning of fossil fuels, a trend expected to rise until the middle of the current century [3]. Therefore, there is an urgent need to find ways to reduce such emissions. Carbon capture and storage (CCS) is one solution that aims at capturing anthropogenic CO_2 for later storage or use, avoiding its emission to the atmosphere. Even though it is not a recent concept, its widespread implementation was, for many years, limited by the high costs associated with the technologies available to perform it [4]. However, many research efforts

have been made in recent years to develop more efficient and, above all, more cost-effective solutions.

The prominent separation technologies predominantly focus on separating CO_2 from other gases at stationary point sources, undoubtedly presenting a major impact on future CO_2 utilization due to the substantial emissions produced by these sources [3]. Such typically encompass major greenhouse gas emitters, such as industrial plants, power plants, and refineries. Sonae Arauco's biomass boiler in Mangualde, developed and operated by CapWatt, uses the best available technology to produce renewable energy from biomass and boost the production process of panels derived from sustainable wood. Wood-based panels are sustainable, flexible, and functional alternatives to all solid wood products, finding many wide-spread applications. This industrial plant can be seen as a stationary point source for CO_2 capture [5]. The plant operates a biomass boiler that uses organic matter as fuel to produce heat or electricity. The biomass centre consumes 300,000 tons of biomass annually, enough to satisfy 100 % of the wood panel plant's thermal energy needs. Additionally, it generates 83 $GWh \cdot year^{-1}$ of decentralized renewable energy, allowing for 90 % of the energy consumed in the factory to be generated from renewable sources [5]. From the boiler's activity, around 90000 $Nm^3 \cdot h^{-1}$of flue gas is produced, at around 165 ºC at 1007 mbar, with CO_2 mass percentage ranging from 13-16 %. Nevertheless, capturing and using this CO_2 can further increase the plant's environmental sustainability, as well as its profitability, if the captured CO_2 is used to produce an added-value chemical like green methanol.

The main goal of this dissertation is to design a process to capture the biogenic CO_2 produced by Sonae's biomass plant in Mangualde, and further purify it to the requirements imposed by a commercial hydrogenation reactor used to produce green methanol. Regular methanol reactors operate between 50 and 100 bar for complete hydrogenation [6]**. Commercially-available CCS technologies will be considered for the capture process, as well as CARBOPORA's unique carbon membrane technology. An industrial process simulator will be used for process design and optimization, allowing for a critical comparison between all technologies to find the most techno-economically viable one.**

1.2 Presentation of the company

This master's thesis was performed through a partnership between two companies, CapWatt and Carbopora. CARBOPORA, LDA is a Portuguese company founded in 2021 with the aim of developing and commercialising membrane-based separation solutions for industrial applications. Being a start-up company from the Faculty of Engineering of the University of Porto (FEUP), CARBOPORA has a strong scientific and technological background supported by more than 20 years of research and development experience in membrane separation

technologies. CARBOPORA capitalises on this knowledge by developing materials and designing gas separation/purification processes using innovative carbon membranes. Its unique membrane technology is made of a green, inexpensive, and renewable polymeric precursor – cellulose – that finds important applications in: (1) O_2-enriched air (critical for oxy-combustion processes); (2) CO_2 capture from flue gas of different origins; and (3) hydrogen (H_2) recovery from hydrocarbon streams.

CapWatt, developed in 2008, is a Portuguese company that operates in the energy sector, responsible for the creation of innovative solutions for energy-related problems. As part of Sonae Capital, it thrives on reducing its carbon footprint by promoting the usage of renewable energies throughout. Today, present in Portugal, Spain, and Mexico has a vast project portfolio and is recognised as an independent energy producer. The company understood the need for a shift towards clean energy thriving to address it by promoting energy-integrated solutions. Since its inception, CapWatt has emerged as a leading company in the sustainable energy sector offering a wide range of clean energy solutions, including carbon capture and storage (CCS) technology, renewable energy sources, and high energy efficiency.

1.3 Organization of the dissertation

The first chapter outlines the project, highlighting the need for solutions to the current climate emergency. It includes a brief presentation of the involved companies and a general description of the objectives to be achieved.

The second chapter is dedicated to a literature review of the state of the art related to different carbon capture and storage technologies, as well as a survey of commercially available purification methods to increase purity.

The third chapter presents the selection of processes to be simulated, in addition to the simulation models used. It also defines the calculation equations and the different parameters for the economic analysis.

The fourth chapter discusses the results obtained through simulations and their economic interpretation regarding CO_2 separation and purification stages.

The last two chapters summarize the main conclusions from the simulated work and include proposals for future research in this field of study.

2. Context and State of the art

2.1 Carbon Capture and Storage

To capture, store and purify CO_2 it is vital to understand the properties of this molecule. CO_2 remains of great interest for capture, as it would benefit the ongoing climate change and global warming. In a case where CO_2 is biogenic, it could also be utilized to produce green by-products with great economic interest. The carbon capture and utilization are optimised if the CO_2 characteristics for specific temperature and pressure values are known. Therefore, analysing the CO_2 phase diagram is of great utility (**Figure 2).** The phase diagram allows us to determine the different stages of CO_2, including its supercritical stage. At this stage, CO_2 exhibits properties of both a liquid and a gas, being neither in its gas nor liquid state but existing in a "supercritical fluid" state [7].

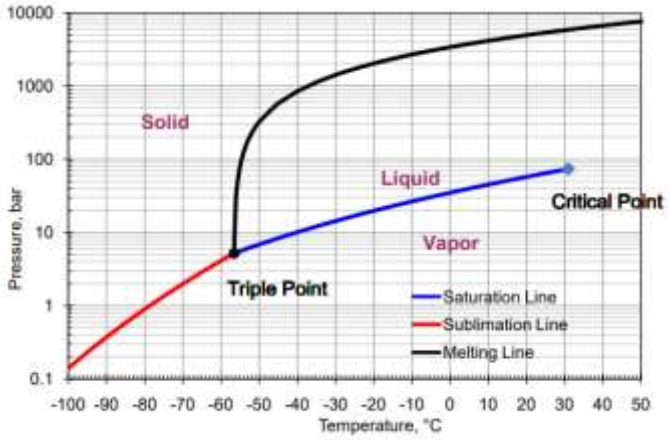

Figure 2. CO_2 phase diagram (Reproduced from [7]).

Understanding the various phases of CO_2 is crucial in determining the appropriate conditions for its separation and purification. When dealing with a CO_2 mixture from flue gas, the presence of oxygen (O_2) is the main impurity, needing an effective purification method. The most effective approach involves condensing the mixture, causing CO_2 to transition into its liquid phase while O_2 remains in its gaseous form, allowing for separation. In the liquid phase, CO_2 can be stored economically within a closed system at ambient temperatures [6].

The captured and purified CO_2 will then be used for the production of green methanol. This is possible using the industrial process of direct hydrogenation with heterogeneous catalysis. The synthesis, favourable at high pressures between 50 and 100 bar, is exothermic and contributes to the reduction of CO_2 emissions. Due to the chemically inert nature of CO_2, a catalyst is needed, with Cu-Zn being the most used one. The overall process reaction is presented in Equation 2.1 [6].

$$CO_2 + 3H_2 \rightleftharpoons H_2O + CH_3OH \quad (2.1)$$

CapWatt defined the entry requirements for the CO_2 reactor at 70 bar, within the mentioned range for the hydrogenation process. CO_2 will be pressurised to this pressure during the purification process and kept at a low temperature for possible storage in its liquid state if needed.

A comprehensive understanding of the CO_2 phase diagram is important to select the best methods for separation and purification. This analysis focuses on maintaining the discussed requirements (CO_2 properties) while exploring different approaches tailored to the specific needs of CCS.

Three main methods are used to capture CO_2 from flue gas. Those are pre-combustion, oxyfuel combustion, and post-combustion. The selection for the most efficient carbon capture technology depends on important factors such as the CO_2 concentration at the flue gas, the type of fuel used during combustion, and the steam pressure [3], [8]. Post-combustion methods are a viable approach for streams with low CO_2 concentration, while pre-combustion methods fare better with high CO_2 concentration streams [8].

2.1.1 Pre-combustion

In the pre-combustion capture method, CO_2 separation and collection occur before the fuel combustion process, mainly through a gasification cycle. Initially, the fuel is gasified inside the reactor by exposing it to a restricted amount of oxygen and heat. This gasification process breaks down the fuel into its constituent components, primarily hydrogen (H_2) and carbon monoxide (CO), forming syngas along with other trace gases that may include carbon dioxide (CO_2) [4]. To produce CO_2 in the gasification process, some conditions need to be ensured, such as increasing the oxygen supply or adjusting the operating parameters. By providing an excess of oxygen relative to the fuel, combustion reactions are promoted, producing CO_2 as a primary output. Alternatively, the syngas can undergo a water-gas shift reaction to convert CO and water to H_2 and CO_2, generating an H_2 and CO_2-rich gas mixture. The latter process concentrates the amount of CO_2 that can be captured and separated. The first large-scale pre-combustion capture plant was constructed in 2012 by Australia's Gorgon natural gas project, capturing 3.4 million tons of CO_2 annually [9].

2.1.2 Oxyfuel

Oxyfuel combustion is one of the most promising technologies for CO_2 capture and storage from existing power plants. This involves the process of burning the fuel with more than 90 % pure oxygen as an oxidant agent instead of regular air to obtain fuel gas rich in H_2O and CO_2. As fuel is burnt directly in pure oxygen, the flame temperature is kept high for this process. Control is performed by recycling CO_2 and H_2O-rich fuel gas directly into the combustion zone. The oxygen is commonly separated from the air using an Air Separation Unit (ASU), which consumes up to

0.6 $kWh \cdot m^{-3}$. Thus, a substantial amount of energy is necessary for the separation process to take place, with nearly 15 % of the electricity generated by power plants dedicated just to powering the air separation units [4]. In the 1990s this process was seen for the first time as a possible carbon capture technology with the Swedish company Vattenfall experimenting with oxyfuel combustion for coal-fired power plants. The first large-scale plant was built in 2008 by this company [10], and its efforts resulted in the oxyfuel processes known today.

2.1.3 Post-Combustion

The most typical process to capture and store CO_2 is the post-combustion method, mainly utilized in natural gas and coal-fired power generation plants. Biomass and other organic resources have emerged as viable alternatives for the combustion process, offering the potential to replace conventional fossil fuels. This process involves burning fuel in contact with air to produce steam, driving a turbine, and generating electricity [6]. The resulting flue gas, referred to as exhaust gas, is primarily comprised of nitrogen (N_2) (over two-thirds), carbon dioxide (CO_2), water (H_2O), oxygen (O_2), and minor amounts of carbon monoxide (CO), nitrogen oxides (NO_x), and sulfur oxides (SO_x) [3]. Due to the relatively low CO_2 partial pressure, the post-combustion approach is the most challenging of the CO_2 capture method. However, it is the most employed method in the industry since it is compatible and easily adaptable to existing processes. From the produced flue gas, CO_2 will be captured and later stored through various possible capture processes [6].

Post-combustion capture method has been a commonly used process for several decades and has undergone significant changes and advancements. While mentioned for decades, it was not until more recently that researchers began exploring the idea of using amine solvents for CCS. Since then, advances have happened with the discovery of more efficient and cost-friendly solvents capable of enhancing the CO_2 capture rate while curtailing energy consumption of the CCS process. In 2000, the first large-scale post-combustion capture plant was built at the Boundary Dam power station in Canada, which captured 90 % of the CO_2 from its flue gas [11].

In post-combustion carbon capture, the method is divided into two different stages. The first stage, known as separation, involves the extraction of constituent gases from the flue gas, including CO_2. The second stage, not always necessary, focuses on purifying the separated CO_2 for subsequent utilisation. Various techniques exist within the separation process to successfully carry out this task. These include the methods of adsorption, absorption, cryogenic distillation, and membrane processes, each possessing its own set of advantages and drawbacks [3]. Likewise, in the context of purification, one may achieve this goal via direct compression or liquefaction.

2.2 Separation Process

There are several separation technologies used for carbon capture and storage. **Figure 2** shows a simplified representation of the most readily available options, all of which are critically analysed in more detail in the following sub-chapters:

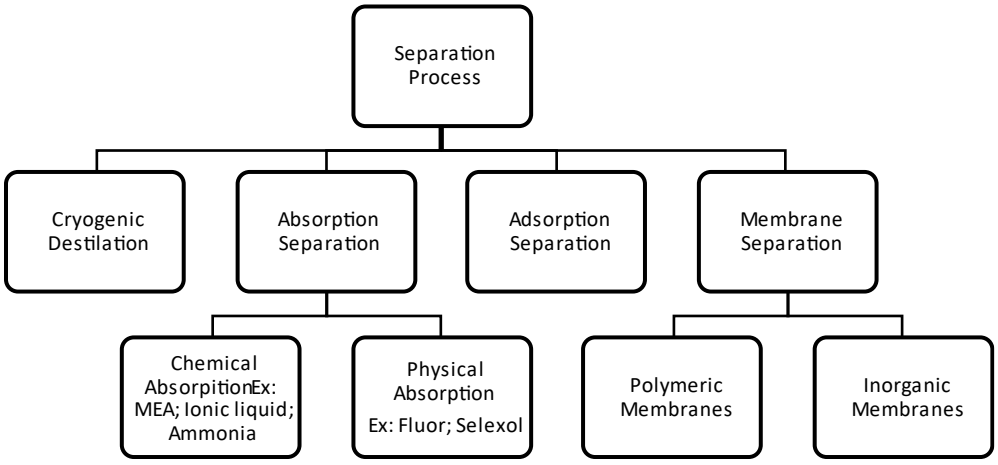

Figure 3. Representation of the different separation processes for CCS.

2.2.1 Separation by Absorption

The absorption separation process is the most mature CO_2 separation technology for large-scale deployment. This process is designed to remove CO_2 from a gas mixture through contact with a selected solvent letting the remaining gases pass through the absorption column. The absorption can be physical or chemical, depending on the selected solvents and the respective intermolecular interactions between gas and solvent [3].

The chemical absorption technique comprises a sequence of steps whereby the flue gas is directed through an absorption and stripping column, with a heat exchanger in between. The absorber usually employs an aqueous alkaline solvent to capture the CO_2, while the stripping unit separates it from the solution. The resultant stream of CO_2 is then refined and made ready for further utilization or storage. The regenerated solvent returns to the absorption column allowing for a continuous cycle. It is worth noting that substantial amounts of thermal energy are necessary to heat the solvent and vaporize the water for stripping the CO_2. Additionally, electric energy is required to compress the flue gas before entering the absorber [4].

Physical absorption is a more straightforward method, requiring a gas-liquid contactor and Flash tanks for solvent regeneration. While the contactor phase happens at higher pressures, solvent regeneration is preferable at lower values or through an increase in temperature [4], [12].

Chemical absorption is the preferred choice of most existing post-combustion plants, as this type of absorption is more economically preferred when the feed CO_2 molar fraction is small, being less expensive than those working with physical absorption. Three common chemical absorption solvents are Monoethanolamide (MEA), Ionic Liquids (IL), and Ammonia, which will be explored in the continuation of the thesis. A schematic representation of the absorption-based separation process plant, independent of the solvent used, is presented in **Figure 4.**

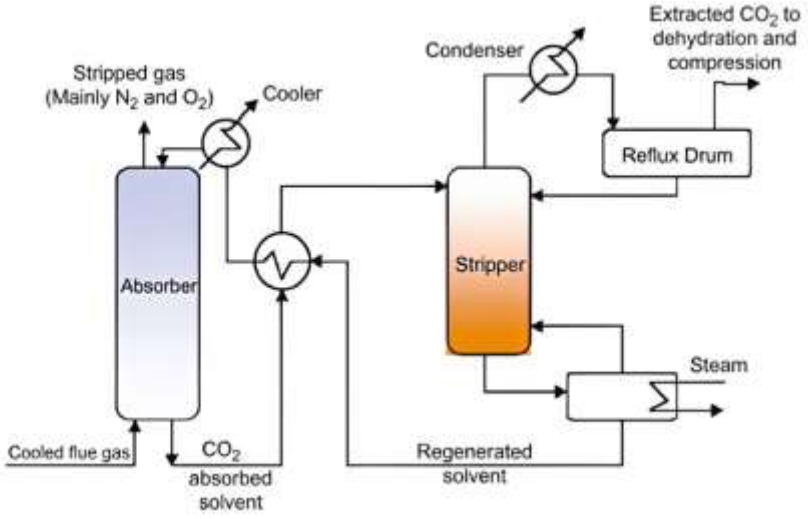

Figure 4. Schematic diagram of a CO_2 absorption plant (Reproduced from [12]).

Monoethanolamine (MEA) solvent

Chemical absorption using Monoethanolamine (MEA) as the solvent remains the most used process for carbon capture due to its fast absorption rate and reasonable volatility [13]. Using MEA as a solvent allows high CO_2 recovery rates and purities of over 98 % [3]. CCS using MEA solvents has had many research efforts and technological developments to improve this technology. Improving the currently available technology aims to reduce costs by 20 % to 30 %. A significant milestone in the history of MEA-based CCS was the construction of the Boundary Dam CCS facility in Canada in 2014. This project was the world's first commercial-scale CCS plant to use post-combustion technology with an amine-based solvent, and it demonstrated the feasibility of CCS as a viable solution for reducing CO_2 emissions [11].

The MEA process begins with feeding the flue gas at the bottom of an absorption tower, while a 20–30 wt % MEA solution is continuously added at the top (Cold Lean MEA). The CO_2 present in the flue gas is selectively absorbed by the solvent (MEA) in an exothermic reaction [14]. Subsequently, the CO_2-rich solvent (Cold Rich MEA) is drained off at the bottom of the absorber and introduced at the top of the stripper after a preheating step in the heat exchanger. In the stripper, Hot Rich MEA desorbs the CO_2 present at high temperatures, and CO_2 lean solvent (Hot Lean MEA) drains the bottom of the column. The regeneration of the amine solvent and concurrent liberation of the CO_2 usually takes place at elevated temperatures (100–140 °C) and

near atmospheric (1–2 bar) pressures. The regenerated amine solvent is recycled back to the absorption tower to continue the cycle [14].

The most common reaction pathway present in MEA absorption processes is the zwitterion mechanism. In this reaction mechanism, the MEA reacts to form zwitterions, which is a molecule that possesses both a positive and negative charge in their constitution - Equation 2.2. This molecule is rapidly neutralized by the existing base in the solution, forming the carbamate – Equation 2.3 [7]. Each mol of MEA solvent captures 0.5 mols of CO_2 [15].

$$CO_2 + RNH_2 \rightleftharpoons RNH_2^+COO^- \tag{2.2}$$

$$RNH_2^+COO^- + RNH_2 \rightleftharpoons RNHCOO^- + RNH_3^+ \tag{2.3}$$

Ionic liquid Solvent

CCS using amine-based solvents is energy intensive and less attractive from an environmental perspective due to emissions of hazardous volatile components. Ionic liquids emerged as a possible solution due to their lower volatility compared with conventional solvents [15], [16].

Ionic liquids are salts consisting exclusively of ions, having a melting point inferior to 100 °C. The first mention of Ionic liquids for gas separation can be traced back to the 1940s. However, little research was done in this area until the late 1990s, when some projects explored the use of ionic liquids in some areas, such as electrochemistry and organic chemistry. Their development continued through the 21st century, broadening its activity area for carbon capture and storage [15]. By using ionic liquid for CCS, it is possible to capture 0.2 mols of CO_2 for each mole of consumed solvent [15], [16].

Ammonia based solvent

Chemical absorption with ammonia as a solvent is widely used for industrial gas sweetening, posing several advantages for carbon capture technology. Compared to MEA, ammonia is a more available solvent with a reduced cost, more resistant to degradation, and requires less heat for regeneration [17]. On the other hand, ammonia solvents have some drawbacks, such as slower kinetics and higher volatility, leading to potentially higher solvent loss. As a result, the absorption is performed at lower temperatures (0 to 10 °C) and the regeneration at higher pressures (2 to 136 bar) [17]. The use of ammonia as a solvent in carbon capture processes has been investigated for several years. It was in 1913 that German chemist Fritz Haber conducted the first ammonia synthesis from nitrogen and hydrogen gases, known as the Haber-Bosch process. After this, more developments occurred, with recent utilization happening for CCS. [18]. The system is operated using an absorber unit to capture CO_2 into a liquid stream followed by a stripper to regenerate CO_2 and the ammonia solution. The reaction process is presented by the following equations [18].

$$CO_2(g) + 2NH_3(\text{aq}) + H_2O(aq) \rightleftharpoons (NH_4)_2CO_3\ (s) \quad (2.4)$$

$$CO_2\ (g) + NH_3(\text{aq}) + H_2O(aq) \rightleftharpoons NH_4HCO_3(s) \quad (2.5)$$

2.2.2 Separation by Adsorption

For this separation process, a physical adsorbent is used instead of a liquid absorbent, contrasting to a chemical absorption process [4]. The separation is based on gas adsorption on solid porous media; in this case, CO_2 is bonded to the surface of an adsorbent. Such process is made possible due to physisorption or chemisorption interactions between the gas molecules and the adsorbent [3]. Physical adsorption has weaker interaction between gas and adsorber, usually Van der Walls bonds, and is typically applied when CO_2 concentration in the feed stream is high, while chemical adsorption has stronger bonds, not being a reversible process [19]

A separation by adsorption process begins by feeding a gas stream bearing CO_2 to an adsorbent-filled column. The CO_2 adheres to the solid surface of the absorbent during the flow saturating it. When the surface becomes saturated with CO_2, it is removed and desorbed through the modulation of temperature or pressure. Two main steps characterise the separation by adsorption. The first step relates to the gas adsorption using adsorber beds. Activated carbons, zeolites, hydrotalcite, calcium oxides, or supported amines make up the principal classes of CO_2 adsorbents. The ideal adsorbent must have fast adsorption/desorption kinetics, high surface area and stability [3], [4]. The second step refers to the regeneration of the adsorbent, where the adsorbates are released [19]. Nowadays, for separation by adsorption, the regeneration process can be executed by TSA (Temperature Swing Adsorption), PSA (Pressure Swing Adsorption), or VSA (Vacuum Swing Adsorption) [3]. A more detailed explanation of these regeneration processes is presented in Appendix A.

2.2.3 Cryogenic Distillation

Cryogenic distillation is a physical separation process based on the condensation of components at very low temperatures. It is a highly similar process to other distillation systems but is mainly used for chemical separations with low boiling points. For this process, a refrigeration system must be combined with the condenser, which must be at the lowest temperature possible [7], [20]. Therefore, the temperature difference between the inlet and outlet of the working fluid in the refrigeration system is as large as possible, leading to high energy consumption [20]. Although there are some examples of its implementation, cryogenic distillation is generally not considered a practical approach to separate CO_2 from flue gas stream due to the high energy costs involved. Another disadvantage is the amount of water required in the feed stream to prevent the formation of ice, which leads to clogged equipment. In short, this approach is not the primary choice for CO_2 separation and will not be considered in this study [20].

2.2.4 Membrane Separation

A membrane can be characterized and defined as a selective barrier between two streams or an interface between two phases [21]. This separation process consists of dividing the feed stream into two specific ones: the permeate stream and the retentate stream. Separation through membranes depends on five mechanisms: Knudsen diffusion, molecular sieving, solution diffusion, surface diffusion, and capillary condensation, with the first two being the leading ones.

Knudsen diffusion occurs when the pore radius is smaller than the mean free path of gas molecules, with molecules striking the pore walls more often than other molecules, then reflected and absorbed in a random direction.

Molecular sieving is a selection based on molecular size when compared to pore size, with larger molecules not being able to pass through the membrane [21]. In a membrane separation, only CO_2 can pass through it while the remaining components are blocked from passage, as shown in **Figure 5.**

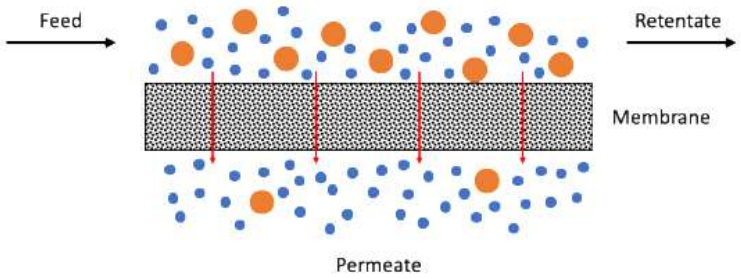

Figure 5. *Scheme of a membrane separation (Reproduced from* [21]*).*

Recently, membrane technology has increased its use in various different industrial applications due to its simplicity, reduced environmental impact, and low energy/cost efficiency compared to other separation processes. Nevertheless, some limitations as fouling, short life, and limited stability have hindered its wider application at a larger scale [3], [22]. For post-combustion processes, where streams present a smaller percentage of CO_2, membrane separation was, for many years, not considered to be the optimal approach [3].

Any membrane used for capturing CO_2 should possess: a marked selectivity towards CO_2 permeation, elevated levels of both thermal and chemical stability, aging resistance, persistent longevity, and an attractive economical cost [3], [4]. Permeability and selectivity are the two factors used to determine and measure the membrane performance. Both depend on the membrane's nature and the conditions it is subjected to, such as temperature, pressure, and gas concentration. Permeability quantifies the permeation of a specific volumetric flow rate of a gas species per unit area of the membrane, subject to a chemical potential difference.

Permeability is usually measured in $mol \cdot m^{-2} \cdot s^{-1} \cdot Pa^{-1}$. Selectivity quantifies the relative preference of the membrane to permeate one gas species over another [23].

Membrane separation technology emerged in the late 60s-early 70s for reverse osmosis and gas separation applications. It has seen continuous growth due to its benefits, such as continuous separation, low energy cost, easy scale-up, and compatibility with other separation processes [21]. The major important contributions of gas separation happened in the late 1970s and early 1980s by multinational Air Products, making gas separation by membrane a competitive device in the industrial field for hollow fibre membranes for nitrogen separation [23]. Membranes are usually characterized according to their chemical nature. These include: Polymeric membranes, inorganic membranes, and even mixed-matrix membranes, being a combination of both polymeric and inorganic materials.

Polymeric Membranes

These are the most used membranes in a variety of industrial processes, as they were the first to emerge and present a combination of acceptable performance factors such as permeability, selectivity, and low cost [3]. The most common polymer materials used for membrane production are cellulose acetate, polysulfone, polyethersulfone, and polyimide [24].

Membranes have recently been more heavily applied for carbon capture. Polymeric membranes have been used in various industrial processes, such as biogas upgrading, gas separation, and natural gas sweetening, all within post-combustion CO_2 capture in power plants and industrial facilities. Studies found that different polymeric membranes have different trade-offs between permeability and selectivity. Finding the right balance between these is quite a challenge.

The most widely used polymeric membranes for Carbon Capture and Storage are those from *Polaris* and *Polyactive*, as both have high values of selectivity and permeance. Of these two, Polaris emerged as the clear favourite for industrial processes [23], [25]. Studies show that the best polymeric membranes use highly selective materials and allow operation at a low-pressure ratio; it should not be neglected the fact that a low-pressure ratio operation is less energy-demanding [23]. While polymeric membranes have low production costs, considerable mechanical resistance, and large-scale production potential, they present low thermal resistance and an insufficient trade-off between permeability and selectivity [22], [25].

Inorganic Membranes

More recently, inorganic membranes started being investigated in hopes of fixing some of the drawbacks found with polymeric membranes, reaching quick success and undergoing rapid innovative development [3]. Contrary to polymeric materials, inorganic membranes possess porous layers that exhibit high surface area and often use metallic or ceramic inert supports to ensure mechanical integrity. These membranes offer advantages such as high resistance to

harsh chemical environments and/or elevated temperatures, exceptional chemical and thermal stability, and extended lifespan. However, their complexity and high fabrication costs have made large-scale production challenging. Such still makes them currently unsuitable for widespread use [3], [22].

Inorganic membranes have also been used for similar applications as polymeric membranes, used as possible substitutes for these. The most common types of inorganic membranes that have emerged are zeolites, ceramic and carbon membranes [26]. More recently, hybrid organic-inorganic membranes, namely the metal-organic framework (MOF) membranes, have emerged. These have a high surface area, adjustable pore structure and good thermal and chemical stability. However, the prepared MOFs usually exist in fine powder form, which makes it difficult to recycle in the industrial field. Carbon membranes surged as a possible competitor for polymeric membranes in various industrial fields, such as Carbon Capture and Storage technologies [27].

2.3 Purification Process

Purification is essential to ensure that the separated gas streams achieve high levels of purity, enabling their practical utilization. By liquifying the resulting gas stream, it helps separate impurities based on their different condensation points. Liquid solutions allow for better and easier storage and transport processes. There are two main paths to achieve highly pure CO_2 grounded in its liquid state: 1) compressed to the preferred pressure through the use of a gas compressor; or (2) liquefied, usually at lower pressures, by using a refrigeration system or Flash separators [28]. Liquid pumps are fundamental to the liquefaction strategy because they increase the pressure with much less electricity and associated lower costs than gas compressors. A schematic representation of both possible paths for the purification and liquefaction of captured carbon is present in **Figure 6.**

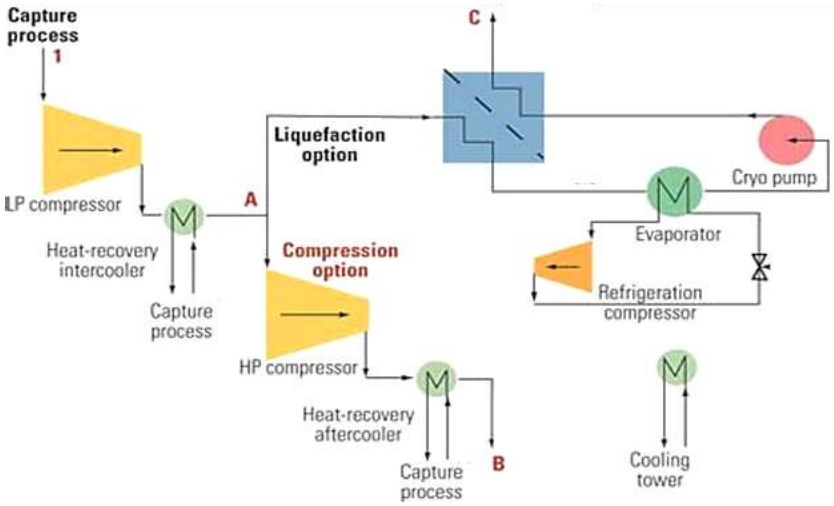

Figure 6. Schematic representation of CO_2 purification process through Compression/liquefaction (Reproduced from [28]).

2.3.1 Purification by Compression

This process is mostly used for streams with high pressure and high CO_2 concentration, mostly for streams produced at industrial plants, like power plants. Compression is associated with greater energy expenditure; therefore, this process should only be used for high-pressure streams, so the pressure increase is not too significant on the overall cost. Through a compressor, the CO_2-rich gas increases its pressure. The compressed gas can also be later dried and cooled through an intercooler to remove moisture and impurities that may or not be present. The CO_2 stream will then be stored in a high-pressure vessel, transported through pipelines, or reused in other industrial processes [28].

2.3.2 Purification by Liquefaction

Liquefaction presents an alternative to purifying and liquefying CO_2 without needing such a high energy demand. To achieve it, it involves cooling the gas to below the value of its critical pressure and temperature, making it liquefy [28]. Liquefaction can be performed using different refrigeration systems. Such can use heat exchangers, compressors, and/or other components to decrease the gas' temperature. Most times, this process is associated with the use of Flash separators. The cost of liquefaction and the energy demand depends on the cooling capacity of the refrigeration system, the temperature of the cooling medium and the gas flow rate. This process, while recent, allow for lower cost and energy demand for the increment of demand for CCS technologies [28], [29]. More recently, the multinational company Air Liquide has performed a process of cryogenic liquefaction as a way to liquefy CO_2. One example of carbon liquefaction after removal from flue gas is the Cryocap™ FG - **Figure 7** [28], [30].

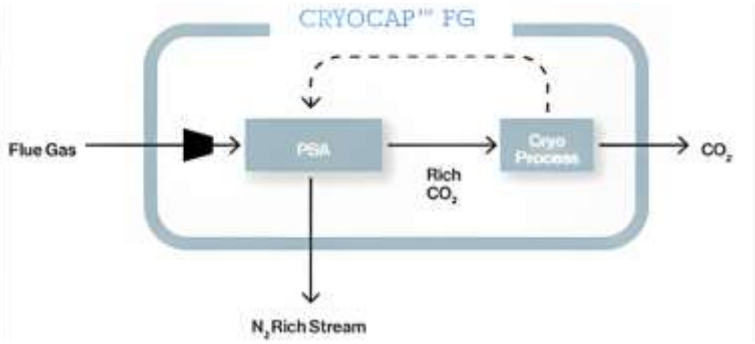

Figure 7. Schematic representation of *Cryocap™ FG* for purification of CO_2 (Reproduced from [29]).

In the Cryocap process, the CO_2 gas is cooled to cryogenic temperatures (up to - 196 ºC), using a cryogenic fluid like methane or nitrogen. The gas will then be compressed to higher pressures by passing through a series of compressors, heat exchangers, or expansion valves, further condensing and cooling the gas [28]. Cryocap uses cryogenic purification to separate the CO_2 stream resulting from PSA. The gas is compressed, dried, and sent to a cryogenic unit, where the CO_2 is separated from the other remaining impurities by a combination of distillation and partial condensation. The non-condensed gases are either recycled back into the process or are removed from the gas stream using centrifuges, filters, or membrane technology [31].

3. Materials and Methods

3.1 CO_2 Capture Process – Case Study

As mentioned, the CO_2 capture process follows two distinct stages: separation and purification. A schematic representation of the different pathways for a complete CCS process is presented in **Figure 8,** demonstrating the possible steps to obtain pure CO_2, from the emitted flue gas.

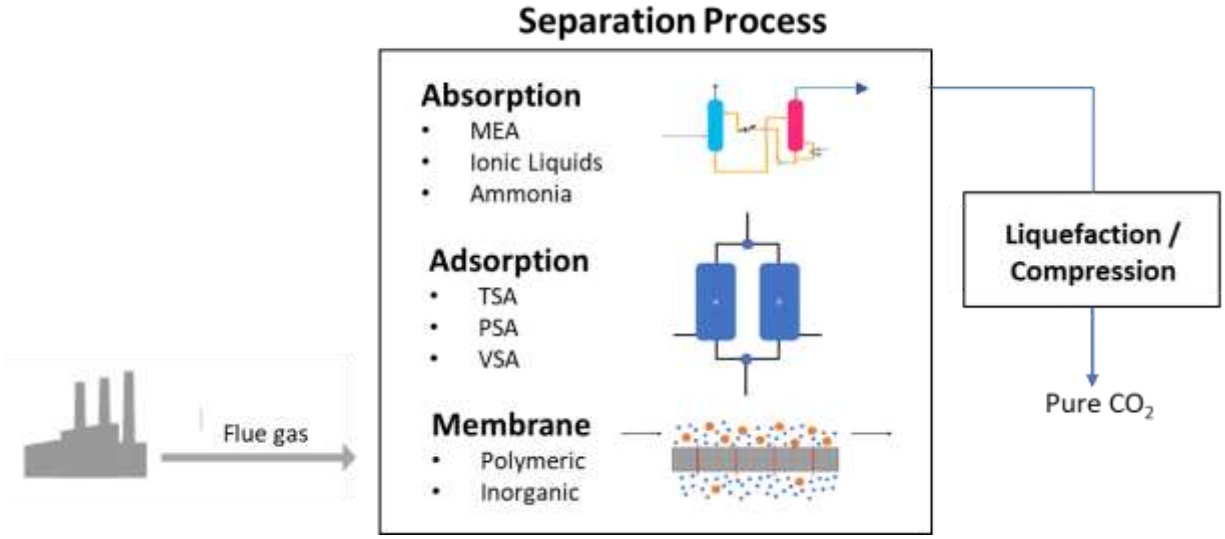

Figure 8. Schematic presentation of the different pathways for a carbon Capture Process.

Within the separation stage, it is crucial to meticulously select the methods employed for simulation purposes, as they directly influence the cost estimation. To assist in deciding which method should be selected, **Table 1** compares the four described separation technologies based on their respective advantages and disadvantages. **Table 21** from Appendix B gives additional information regarding the selection process. The collected data suggest that membrane separation has emerged as the most economically viable process. Therefore, it represents a strong contender that aligns with the defined objective of enhancing Carbopora's role in CCS technologies. The adsorption process is not a viable alternative due to its high cost, with difficulty reaching purities above 95 %. Absorption is an interesting selection due to being the most used industrial process (with MEA solvent) for any CCS technology. Therefore, membrane separation and Absorption with MEA solvent were chosen as the separation technologies for further study. After deciding on the best separation methods, the next step is to determine how to simulate and evaluate them. With this, several models are employed to predict the respective separation and purification behaviours in order to achieve a complete comparison study on the best CCS technology for a flue gas mixture. A cost model was also developed to determine the economic feasibility of these technologies based on the modelling results.

Table 1. Advantages and Disadvantages of the studied separation processes.

Technology	Type/solvent	Advantages	Disadvantages	Ref.
Absorption	MEA	1. Cheap solvents 2. Fast absorptivity 3. Strong CO_2 abs. capacity	1. High energy consumption 2. Equipment corrosion 3. Prone to O_2 and thermal degradation	[32]
	Ionic liquids	1. High solubility and selectivity 2. Environmentally friendly 3. High thermal and chemical stability 4. Low regenerative energy demand 5. No equipment corrosion	1. High viscosity and low mass transfer rate of CO_2 2. Only used in the laboratory	[32]
	Ammonia	1. No equipment corrosion 2. Low energy consumption 3. Strong absorption capacity	1. Volatile 2. Resulting in the waste of resources and the loss of energy due to overproduction of fertilizer	[32]
Adsorption	PSA	1. Environmentally friendly 2. Fast return on investment	1. Requires re-packing of the adsorbent sieve material every 3–5 years 2. Higher complexity 3. Higher energy cost compared to VSA	[33], [34]
	TSA	1. Volume of flue gas at ambient pressure does not need pressurization. 2. Waste heat is utilized to supply energy for temp. swing 3. Does not require compression or usage of vacuum	1.Higher energy associated with the repeated heating and cooling 2. Longer regeneration time 3. need of large volumes of hot non-adsorbing purge gas for regeneration	[33], [34]
	VSA	1. Extended use of the adsorbent 2. Process simplicity 3. Low energy consumption and cost 4. Less susceptible to dust deposits in adsorbent bed 5. Reduced maintenance	1. High sensitivity to the flue gas impurities 2. Low capacity of sorbents	[33], [34]
Membranes	Polymeric	1. Low cost 2. Ease of fabrication 3. Flexible and lightweight 4. good selectivity	1. Fouling 2. Low chemical resistance 3. Lower tolerance for pH	[22]
	Inorganic	1.Able to withstand high temperatures and harsh chemical environments 2. Stability 3. Higher selectivity	1. Low membrane surface per module volume 2. Fragile 3. Lower CO_2 permeability 4. More expensive	[22]

3.2 Development of the gas permeation model

In order to predict membrane separation performance for both polymeric and inorganic membranes, a gas permeation model was developed to assess the results. **Figure 9** presents a scheme of a membrane, including the feed stream (F_F), retentate stream (F_R), permeate stream (F_P), the flux (J_i) that permeates across the membrane.

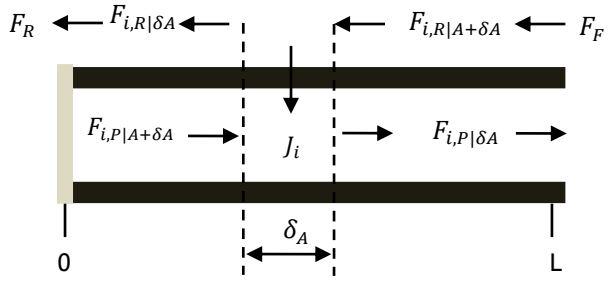

Figure 9. Illustrative ideal membrane separation process configuration with the respective mass balance at an infinitesimal area.

Based on **Figure 9**, the following equations (Equations 3.1-3.10) analyse the molar fraction distribution, area calculations, and the impact of pressure differentials on molar flow rates. The differentiation of these equations allows for the construction of the model. A counter-current membrane model with a multi-component feed was developed by dividing the membrane into *n* perfectly mixed stages with equal areas. The model is based on the molar balance for the infinitesimal area element on the retentate side, using the membrane length (from 0 to L). These equations describe the molar flow of the component '*i*' in the retentate changes as one considers continuously smaller elements along the membrane. This way, the change in molar flow rate of component '*i*' per unit area equals the flux across the membrane.

$$F_{i,R|A+\delta A} - F_{i,R|A} = J_i \cdot \delta A \tag{3.1}$$

$$\lim_{\delta A \to 0} \frac{F_{i,R|A+\delta A} - F_{i,R|A}}{\delta A} = J_i \tag{3.2}$$

$$\frac{\mathrm{d}F_{i,R}}{\mathrm{d}A} = J_i \tag{3.3}$$

Normalizing the spatial variable (*z*) by the membrane length (*L*) (Equation 3.4) the membrane area (*A*) can be expressed by Equation 3.5 with *r* being the membrane radius. The retentate flux can be written as follows presented in Equation 3.6, where $\mathcal{L}_i$ is the membrane permeance.

$$x = \frac{z}{L} \tag{3.4}$$

$$dA = 2\pi r dz = 2\pi r L dx = A \cdot \mathrm{d}x \tag{3.5}$$

$$dF_{i,R} = \mathcal{L}_i \cdot \left(P_R \cdot x_{i,R} - P_P \cdot y_{i,P}\right) \cdot A \cdot \mathrm{d}x \tag{3.6}$$

P_R and P_P are the permeate and retentate stream pressures respectively, $x_{i,R}$ and $y_{i,P}$ are the

mole fraction of component *i* in the retentate and permeate stream respectively. The stream that flows across the membrane is counter-current, inducing the permeate mass balance to be equal to the retentate mass balance.

$$\frac{dF_{i,P}}{\mathrm{d}x} = \frac{dF_{i,R}}{\mathrm{d}x} \tag{3.7}$$

$$dF_{i,P} = \mathcal{L}_i \cdot \left(P_R \cdot x_{i,R} - P_P \cdot y_{i,P}\right) \cdot A \cdot \mathrm{d}x \tag{3.8}$$

With these, there are two differential equations for each component, one for the retentate and the other for the permeate, therefore two boundary conditions are necessary to obtain and solve the system of differential equations.

$$z = 0 \qquad F_P = 0 \rightarrow y_{i,P} = 0 \tag{3.9}$$

$$z = 1 \qquad F_F = F_R \rightarrow x_{i,F} = x_{i,R} \tag{3.10}$$

Based on the defined equations, the model is developed through *Python* language, by applying the *bvpBC* function to define boundary conditions and the *bvpSED* function being used to solve boundary value problems for ordinary differential equations (ODEs). The advantage of developing the gas permeation model through *Python* is that not only is innovative (as the best author knowledge, this is the first membrane simulator model solved in this programming language), but it is also open-source, meaning that the programming language is freely available and can be modified, accessed, and distributed by anyone. It is versatile, easy to learn, and allows for easy integration with other computer languages such as Java and C++.

3.3 Simulation with Aspen Plus

Aspen software was used to simulate the separation process through absorption using MEA as solvent. This software is also used for the purification process of the non-purified gas stream that leaves the MEA absorption process and the membrane separation process. Aspen Plus is a computer-aided simulation and chemical process optimization software. It is mainly used for engineering calculations and simulations. Aspen focuses on upgrading existing processes, designing new ones, or improving the overall performance. The produced Aspen software models are based on knowledge of technical processes, incorporating technological innovations, and providing reliable results tested in real industrial plants. In the simulation, process parameters and flow diagrams are employed to predict the output results. It employs material and energy balances, thermodynamic equilibrium, and rate equations to provide information about process performance, such as the conditions, properties, and equipment sizing [4]. Aspen software uses three simulating components. The first one, properties, provides a database of both physical and thermodynamic properties of the chemical components used in the process. The performance of the purification process was analysed through the usage of different

thermodynamic models. The best performance was determined to be Predictive Soave-Redlich-Kwong (PSRK), as it minimised the presence of azeotropes and gave accurate Phase Equilibrium Predictions. The second one, simulation, presents the process flow diagram, and the input parameters desired to simulate the process. The third one is the Energy Analyser, used to analyse and optimize the heat transfer and energy consumption of the simulated process. It provides information, such as the power requirements of heat exchangers based on heat duty and temperature profiles, as well as detailing the utility requirements for the process.

3.4 Cost model and equipment sizing

For any industrial separation process, it is essential to consider both the capital expenditures (CAPEX) and the process operating expenditure (OPEX). CAPEX combines the process investment required, including the infrastructure, installation, and equipment costs. OPEX relates to the ongoing operational expenditure necessary for the specific process. This includes all raw material inputs, energy consumption, labour work, and maintenance.

A regular CCS by absorption process requires the use of heat exchangers, pumps, and an absorber and reboiler columns. From the used heat exchangers, only one is selected to determine its respective cost through Equation 3.11. All other heat exchangers' costs are determined through Equation 3.12, which determines cost by comparing the heat duty of both exchangers. The chosen heat exchanger for Equation 3.11 should demonstrate a balanced heat transfer capability, ensuring that the cumulative cost of all heat exchangers remains within an optimal range. All heat exchangers are admitted as shell-and-tube, with *A* being its area. All costs are determined in euros (€).

$$C_h = e^{11.147 - 0.9186 \cdot \ln(A) + 0{,}0979 \cdot \ln(A)^2} \tag{3.11}$$

$$Cost\ of\ heat\ exchanger\ A = Cost\ of\ heat\ exchanger\ B \cdot \left[\frac{heat\ duty\ of\ A}{heat\ duty\ of\ B}\right]^{0.6} \tag{3.12}$$

The cost of both columns' separators, absorbers and reboiler ($C_{separator}$) is computed through its weight (*W*) in kg, internal diameter (D_i), height (*h*), wall thickness (*t*) (all three in meters) and fluid density (ρ), in kg·m^{-3} [35]. $C_{separator}$ depends on the material factor (F_M), cost of the empty equipment (C_v) and the additional cost of platforms and stairs (C_{PL}).

$$W = \pi \cdot (D_i \cdot t) \cdot (h + 0.8 \cdot D_i) \cdot t \cdot \rho \tag{3.13}$$

$$C_v = e^{7{,}0374 + 0{,}18255 \cdot \ln(W) + 0{,}02297 \cdot \ln(W)^2} \tag{3.14}$$

$$C_{PL} = 237{,}1 \cdot D_i^{\,0{,}63316} \cdot L^{0{,}80161} \tag{3.15}$$

$$F_M = 1$$

$$C_{Separator} = F_M \cdot C_v + C_{PL} \tag{3.16}$$

For a membrane separation process, the necessary equipment are compressors and vacuum pumps to create the driving force that allows the permeation to occur. The power duty (P_C) for each equipment is determined by Equation 3.17, where η_C is the compressors and vacuum pump's efficiency, Q is the flow rate passing through the equipment in mol·s^{-1}, R is the ideal gas constant in J·K^{-1}·mol^{-1}, T is the temperature in Kelvin and γ is the heat capacity ratio [35].

$$P_C = \frac{1}{\eta_C} \cdot \frac{\gamma}{\gamma - 1} \cdot QRT \cdot \left[\left(\frac{P_F}{P_{ent}}\right)^{\frac{\gamma}{\gamma-1}} - 1 \right] \tag{3.17}$$

Compressors and vacuum pumps costs are determined by Equations 3.18 and 3.19, respectively, with the cost of regular pumps being determined by a correlation graph in Annex A – **Figure 32**:

$$C_{compressor} = e^{7,2223+0,8 \cdot \ln(P_C)} \tag{3.18}$$

$$C_{vacum\ pump} = 150000 \cdot \left[\frac{Q}{5250}\right]^{0.6} \tag{3.19}$$

For the purification process, the needed equipment is Flash separators. This cost is reflected in Equation 3.16, with C_{PL} and C_v determined as follows for these Flash separators [35]:

$$C_v = e^{8,717 - 0,233 \cdot \ln(W) + 0,04333 \cdot \ln(W)^2} \tag{3.20}$$

$$C_{PL} = 1,58 \cdot {D_i}^{0,20294} \tag{3.21}$$

The cost of membrane modules ($C_{Membrane}$) is defined based on the total area used in m^2 (A_T) and the unit cost of a membrane module (K_M) in €·m^{-2}

$$C_{membrane} = A_T \cdot K_M \tag{3.22}$$

Equipment cost ($C_{equipment}$) refers to the total cost of the equipment used. CAPEX refers to equipment expenditure, including an additional 20 % to account for non-scaled items such as valves and mixers.

$$CAPEX = 1.2 \cdot (C_{equipment}) \tag{3.23}$$

To determine the annual expenditure for CAPEX cost, it is necessary to determine the Estimated Annual Cost (EAC), which depends on CAPEX value. CAPEX determined from the Equation 3.23 does not consider additional costs, such as installation, piping and construction. Therefore, Equation 3.24 determines the EAC considering OPEX as 53 % of the overall EAC value [35].
Table 2 defines the needed parameters to determine EAC with Equation 3.24.

$$EAC = \left[\frac{CAPEX}{0.53} + \frac{CAPEX}{0.53} \cdot A \cdot (1 - A)^{-1}\right] \cdot B \cdot ((1 - (1 + B))^C \tag{3.24}$$

Table 2. Parameters used to determine EAC with Equation 3.24.

Parameters	Definition	Value	References
A	Working Capital	15 %	[35]
B	Interest Rate	10 %	
C	Active years	15 years	

To determine the OPEX value, it is necessary to calculate the energy costs for each process. Energy costs, related to the utilities, are **steam, cooling water, refrigerant liquid, electricity, and hot oil**. C_{steam} was defined as 2 €·MMBTU^{-1}, as this is the value on the Aspen Plus library for a similar separation process for CCS from flue gas. The following equations indicate the energy calculations in €·year^{-1} for electricity (C_E), hot oil (C_{HO}), steam (C_S), cooling water (C_{CW}), and refrigerant liquid (C_{RL}), with **Table 3** showing their respective cost parameters. P_i represents the power requirement for each utility with t_{op} being annual operating time.

$$C_E = C_{eletricidade} \cdot P_C \cdot t_{op} \tag{3.25}$$

$$C_{HO} = C_{hot\ oil} \cdot \frac{P_1}{VLH} \cdot t_{op} \tag{3.26}$$

$$C_{CW} = C_{cooling\ water} \cdot P_2 \cdot t_{op} \tag{3.27}$$

$$C_{RL} = C_{refrigerant\ liquid} \cdot P_3 \cdot t_{op} \tag{3.28}$$

$$C_S = C_{steam} \cdot P_4 \cdot t_{op} \tag{3.29}$$

Table 3. Definition and value for the parameters needed for OPEX calculations.

Parameter	Value	References
$\boldsymbol{t_{op}}$	8000 h·year^{-1}	-
$\boldsymbol{C_{eletricity}}$	0.08 €·kwh^{-1}	[36]
$\boldsymbol{C_{hot\ oil}}$	0.404 €·m^{-3}	[37]
Natural gas VLH	8744.1 kcal·m^{-3} PTN	[38]
$\boldsymbol{C_{cooling\ water}}$	0.05 €·m^{-3}	[39]
$\boldsymbol{C_{refrigerant\ liquid}}$	23.08 €·GJ^{-1}	[40]

All costs are updated with the *Chemical Engineering Plant Cost Index* (CEPCI) and cost indexes, to reflect current prices. OPEX, apart from energy spending, considers material supply (0.5 % of the EAC), and labour cost (10 % of the yearly workforce expenditure). All simulations consider a work team of 16 employees and 4 supervisors. The employees' salary is defined as twice the minimum wage, with a 25 % increase for night shifts. The supervisor's salary is defined as thrice the minimum wage for the same increase [35]. Therefore, the whole process cost is given by:

$$C_{process} = \frac{EAC + OPEX}{Recovered\ ton\ of\ CO_2} \tag{3.30}$$

4. Results and Discussion

This project aims to design a process to capture the biogenic CO_2 produced by Capwatt's biomass plant in Mangualde, and further purify it to the requirements imposed by a commercial hydrogenation reactor used to produce green methanol. Commercially-available CCS technologies will be considered for the capture process, as well as CARBOPORA's unique carbon membrane technology. The design and performance of the separation and purification stages of the proposed CCS processes heavily depend on the flue gas conditions emitted from the biomass plant. The simulations are performed considering an initial stage of gas pre-treatment where impurities (components below 1% in the mixture) are removed. The gas mixture conditions used for simulations are listed in **Table 4.**

Table 4. Flow rate composition for flue gas post pre-treatment.

	Mixture
Flow rate (mol·s^{-1})	687.27
Molar percentage of CO_2 (%)	14.5
Molar percentage of O_2 (%)	7.9
Molar percentage of N_2 (%)	77.6
Temperature (ºC)	165
Pressure (bar)	1

These flue gas conditions were used as the feed stream in all the simulations, allowing for a simple and fair comparison between processes. In addition, a **threshold** for both CO_2 recovery and purity was set by the two partner companies to be competitive; the purity after the separation process should reach at least 95 % to be then possible to increase it to 99.9 % at the purification stage, while the CO_2 recovery, should be between 80-85 % after the separation process to ensure an end recovery of 80 % after the purification stage.

4.1 CO_2 Separation by Absorption with MEA solvent

The CO_2 separation by Absorption with MEA solvent was designed and simulated with the Aspen Plus V12 simulator. As illustrated in **Figure 10**, the process begins with the flue gas entering the bottom of the absorber column. At the same time, the solvent is introduced at the top, allowing for a counter-current reaction inside the equipment. Water and MEA mixture work as the solvent. As 1 mol of MEA can recover 0.5 mol of CO_2, and there are 100 mol·s^{-1} of CO_2 present in flue gas, the absorption process will require 200 mol·s^{-1} of MEA. Most of these processes have an optimum solvent concentration of 20-30 % of MEA, with the rest being water,

requiring a water flow rate of 466.67 mol·s^{-1}[4]. Therefore, the solvent flow rate is 666.67 mol·s^{-1}, which means a 1:1 ratio between the flue gas and solvent. The rich solvent stream exits the bottom of the absorber column at 1.05 bar and is pumped to 1.1 bar using Pump 1; and, heated in Heater 1, reducing the stream temperature to 50 ºC before entering the stripper column. In the stripper column, the rich solvent stream is heated using steam. Steam causes the absorbed CO_2 to be driven off, leaving from the top of the column at ambient pressure. Water vapor is also removed from the top and pumped back into the absorber column. The bottom-stream, containing recovered MEA solvent, exits on the bottom of the stripper at 105 ºC and is cooled in Heater 2 to 100 ºC. This stream is then mixed with water and pure MEA, undergoing further cooling, and being pumped before re-entering the absorber column at 90 ºC and 1.08 bar. These solvents react with the flue gas inside the column, restarting the process. The overall process operates as a closed cycle, with energy consumption attributed to steam heating in the reboiler, electricity usage in the three pumps, air consumption in the three heaters, and a refrigerant liquid in the condenser. Air is not considered in terms of energy consumption due to its readily available and low-cost nature. The reboiler column's condenser employed a coolant capable of achieving temperatures close to -25 ºC.

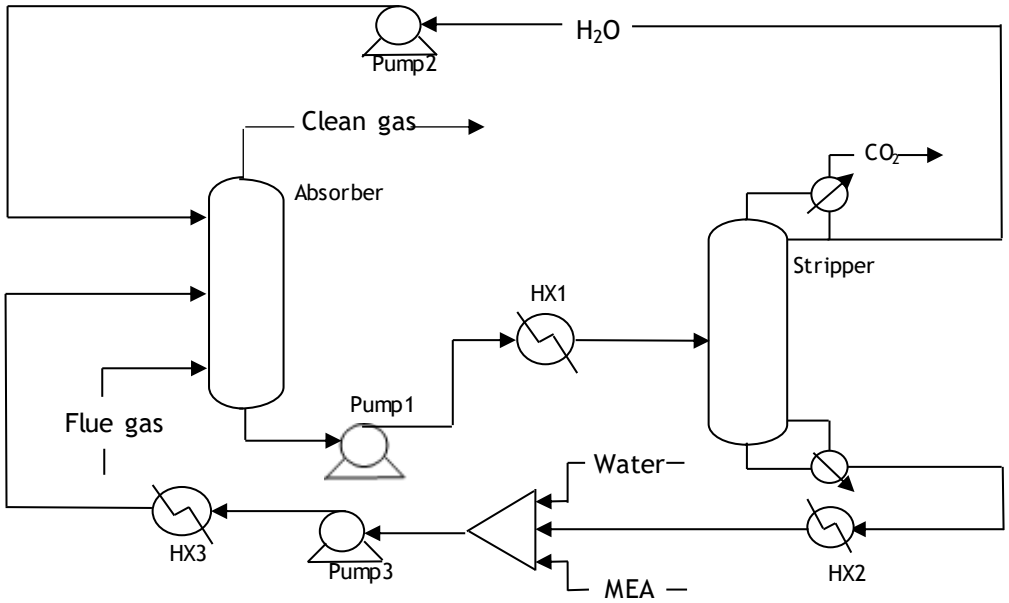

Figure 10. Schematic of the separation process through absorption using MEA as solvent.

The absorber column was simulated with two sections. With a total of 30 stages, the first section being from stages 1 to 5, with a diameter of 4 meters and a height of 3 meters. The second section goes from stage 6 to 30, with a diameter and height of 5 meters. The stripper column has a total of 20 stages with a diameter of 5 meters and a height of 8.2 meters. The reboiler column works in a rate-based performance, being designed to provide constant and controlled heat input to the bottom section (reboiler section) of the stripper column and allowing control of the process stability and energy efficiency. Due to the solvent recovery in

the stripper column, only a one-time purchase of MEA will be needed, with a secure value for potential losses. Aspen Plus determines this value as the total accumulated quantity in circulation. In this case, 1147 mols of MEA were needed. To ensure a sufficient amount of MEA, a 20 % higher quantity than the amount needed for the process (1376.4 mols) was purchased at a cost of 1.62 €·kg^{-1} [39]. The separation performance of the previously-described CO_2 separation process through MEA absorption is displayed in **Table 5**.

Table 5. Results obtained from the separation process through absorption with MEA solvent.

	CO_2 Purity (%)	CO_2 Recovery (%)	Pressure (bar)	Temperature (ºC)
Absorption Process with MEA	98.9	88.9	1.00	4.08

The process recovered a high percentage of the CO_2 from the flue gas at a high purity of 98.9 %. The results of the overall cost regarding the simulated absorption process with MEA solvent are presented in **Table 6.**

Table 6. Overall expenditure results concerning absorption process with MEA solvent.

	Cost values
Solvents (€·year^{-1})	5347.5
Maintenance Cost (€·year^{-1})	2025.9
Pumps power (kW)	5.17
Electricity consumption (€·year^{-1})	3306.1
Reboiler duty (cal·s^{-1})	2.35×10^7
Steam consumption (€·year^{-1})	5.37×10^6
Refrigerant consumption (€·year^{-1})	3.52×10^6
Energy Cost (€·year^{-1})	8.89×10^6
EAC (€·year^{-1})	1.15×10^6
OPEX (€·year^{-1})	9.62×10^6
Overall Cost (€·tonCO_2^{-1})	86.83

The total specific cost is estimated to be 86.83 €·tonCO_2^{-1}, a value on par with similar processes found in the literature (**Table 21 – Appendix B). Figure 11** plots the data found in **Table 6** to better interpret the results. As it can be seen from **Figure 11A**, energy consumption associated with utilities is the most relevant contributor to the overall cost of the process. Steam and

coolant make up the vast majority of energy spending. Electricity has almost no impact on energy costs due to the extremely low energy duty associated with the three pumps. Nevertheless, the high energy consumption associated with this process (82.5 %) may undermine its cost-effectiveness. In this regard, separation processes based on membrane technologies might be more competitive, as discussed in the next sub-chapter.

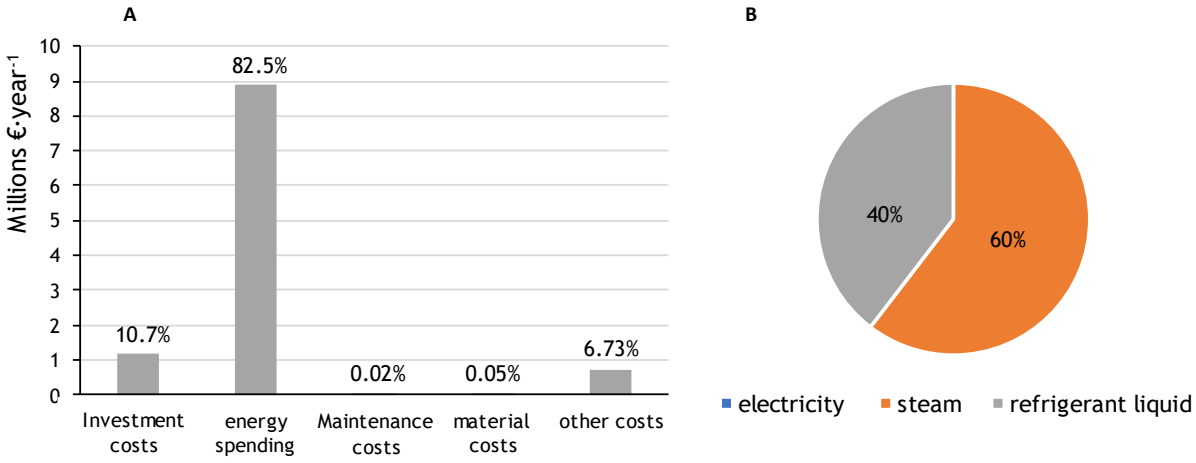

Figure 11. A) Cost distribution for the simulated absorption process, and B) distribution of the energy spending for the process.

4.2 CO_2 Separation with Membrane Technology

4.2.1 Model validation

As Aspen Plus is not capable of correctly simulating membrane separation, this technology requires the use of a mathematical model to correctly predict gas separation across the membrane modules. The developed method was validated through comparison with two literature models for membrane separation, the Mollocator and Chembrane, and a third previously "in-house" developed model implemented in MATLAB. The Chembrane simulator uses the successive stages method to solve a set of differential equations. The Mollocator method obtained its results using orthogonal collocation, being the only method to consider pressure drop [41].

The developed Python code, and the "in-house" MATLAB code use a more straightforward available tool that simulates the membrane separation process by solving the system of differential equations described in subchapter 3.2. In order to validate the developed Python model, the simulation results were compared to the three other mentioned membrane simulators for the same input values. Therefore, for each model it was determined the retentate and permeate flow and respective CO_2 purity. The comparison is listed in **Table 7** with the respective deviations between the models [41].

Table 7. Comparison of simulation models.

	Permeate flow ($mol \cdot s^{-1}$)	Permeate CO_2 purity	Retentate flow ($mol \cdot s^{-1}$)
Chembrane	0.0300	59.88 %	0.3200
Mollocator	0.0293	60.34 %	0.3197
MATLAB	0.0306	60.59 %	0.3199
Python	0.0303	60.30 %	0.3197
Deviation from Chembrane	1.00 %	0.70 %	0.09 %
Deviation from Mollocator	3.41 %	-0.07 %	0.00 %
Deviation from MATLAB	-0.98 %	0.48 %	0.06 %

The developed Phyton simulator has comparable results to models reported in the literature, with the largest deviations observed in the permeate flow rate. There is a deviation of 3.41 % from the Mollocator simulator due to considering load losses, but it remains below the acceptable limit of 5 %. For the other results, the deviation of the developed simulator is below 1 %. Therefore, the developed simulator accurately describes gas separation in a membrane module through user-friendly software. Contrary to most of the simulators found in the literature that rely on complex numerical methods, the developed simulator offers a simple approach with comparable results.

4.2.2 Polymeric Membranes

The developed membrane CCS processes were performed in Phyton. To simulate the separation and perform an overall cost analysis, some parameters must be defined (**Table 8).**

Table 8. Polymeric membrane performance parameters (Reproduced from [42]).

	Membrane Parameters
Permeance to CO_2	2200 GPU
Permeance to O_2	220 GPU
Permeance to N_2	44 GPU
Membrane Cost	50 $€ \cdot m^{-2}$

Other parameters, such as permeate/feed pressure and membrane module area, directly depend on the configuration of the membrane process itself, making it necessary to define in order to reach the desired results. Therefore, the first step will be to determine the optimal configuration and number of stages.

Polymeric Membranes – Influence of the overall configuration

One to three stages were considered for this process, to ensure technological feasibility and optimal cost-effectiveness. All three scenarios were simulated and configurated in series for a feed pressure of 5 bar, all in the presence of vacuum at the permeate side. In order to minimize overall costs, the feed pressure for both the second and third stages was considered as 1 bar.

For all three cases, the membrane areas were optimized to guarantee the best results that conformed to the defined thresholds. The stage number influence on overall membrane separation performance is shown in **Table 9**. As it can be observed, it is mandatory to configure three membrane stages to obtain the desired CO_2 recovery and purity.

Table 9. Stage number influence on overall membrane separation performance.

Number of stages	Feed pressure stage 1(bar)	Permeate pressure all cases (bar)	Feed pressure stage 2 (bar)	Feed pressure stage 3 (bar)	Recovery (%)	Purity (%)
1	5	0.1	-	-	93.1	65.1
2	5	0.1	1	-	89.3	91.3
3	5	0.1	1	1	87.4	97.5

In terms of configuration, 4 different ones were evaluated: one without any recycle (Configuration A - **Figure 12**), two with recycle coming from the retentate stream of membrane module 3 (Configuration B and C – **Figure 33** and **Figure 34** in Appendix C) and, one with recycle coming from the retentate stream of membrane module 2 (Configuration D – **Figure 35** in Appendix C). As expected, the configuration influences the overall membrane separation performance, as presented in **Table 10.** Only configuration A, without recycling, results in the desired recovery and purity, as mentioned in section 4. In addition, configurations B to D also have the disadvantage of increasing the flow rate through the compressors and pumps, increasing the overall process costs. Therefore, configuration A was chosen for the simulation scenarios later discussed – **Figure 12.**

Table 10. *Configuration influence on overall membrane separation.*

Configuration	Recovery (%)	Purity (%)
A	87.4	97.5
B	91.9	93.9
C	92.9	94.3
D	93.3	94.2

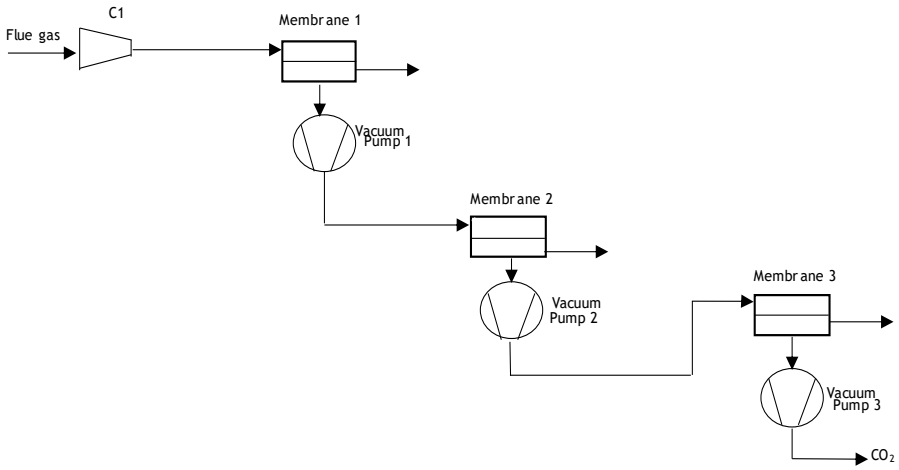

Figure 12. Schematic representation of the best configuration for the separation process using membrane technology.

Polymeric Membranes – Influence of feed pressure

Having chosen the optimal configuration, the next step was to optimize the pressure ratio at each one of these stages. As previously stated, this pressure ratio will dictate the membrane area required for each stage in order to reach the threshold values for CO_2 recovery and purity. In membrane separation technology, the relationship between permeate and feed pressure is crucial for the success of the process. This ratio determines the separation driving force. While a higher ratio is desirable, it also leads to an increment in energy consumption. To address this challenge, vacuum is employed on the permeate side of all three stages to enhance the driving force without significantly raising the feed pressure. A feed pressure range from 1.2 bar to 5 bar is considered at stage 1. Aiming to minimise all the energy costs and simplify the overall simulation procedure, the second and third stages' feed pressure were all set to be at 1 bar. **Figure 13** shows the results of the total membrane area of all stages simulated as a function of CO_2 recovery and purity. **Figure 14** simulates a similar behaviour regarding overall cost.

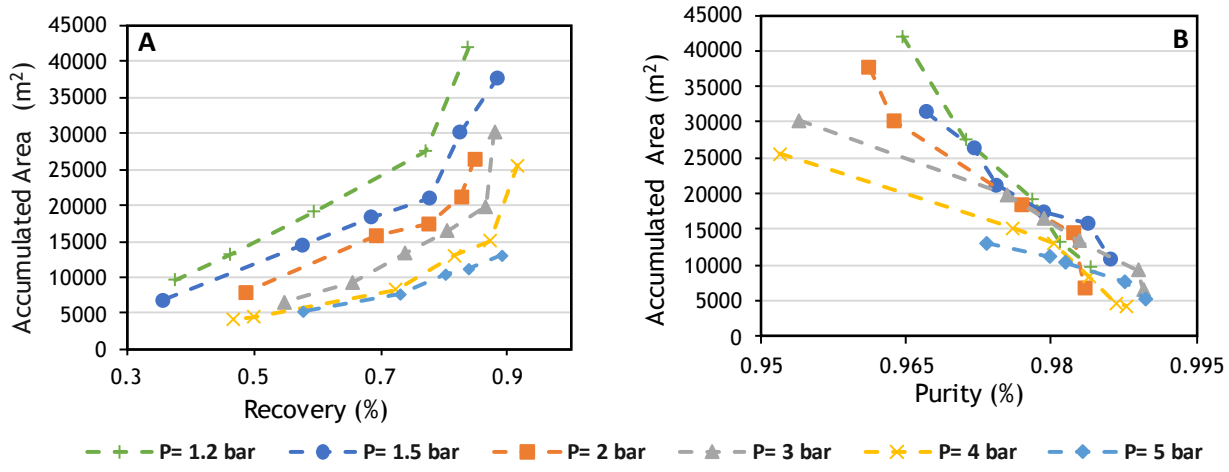

Figure 13. A) Relation between recovery and accumulated membrane area, and B) Relation between purity and accumulated membrane area for various feed pressures with 3 polymeric membrane stages.

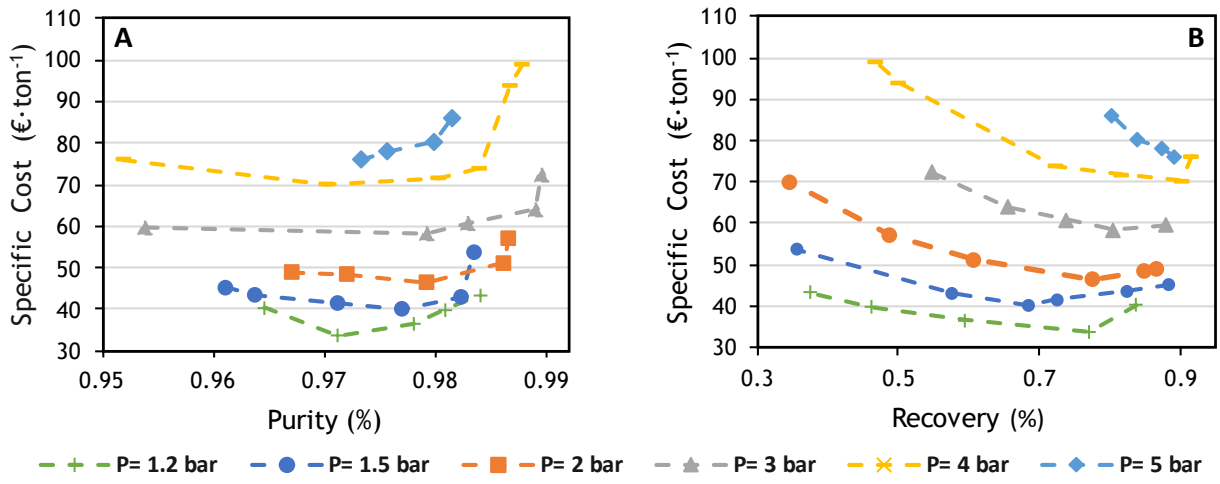

Figure 14. A) Relation between recovery and accumulated membrane area, and B) Relation between purity and accumulated membrane area for various feed pressures with 3 polymeric membrane stages.

As seen in **Figure 13A,** achieving higher recovery rates requires larger membrane areas. This is because an increased area provides a larger surface for the solute to pass through the membrane. On the other hand, this increase in solute permeation decreases the CO_2 purity, as shown in **Figure 13B**. In both cases of **Figure 13**, it is evident that lower feed-to-permeate pressure ratios require larger membrane areas to achieve the same recovery and purity values as the cases with higher pressure ratios. A higher-pressure ratio means a higher driving force; therefore, less membrane area is needed to achieve its purpose. **Figure 14A** and **Figure 14B** display the overall impact that recovery and purity have on the overall process cost. Additionally, in **Figure 14,** a higher-pressure ratio leads to higher specific costs, due to an increase in energy consumption that remains the major cost contributor.

One can observe an inflection point for recovery and purity concerning the specific cost for all studied feed pressure scenarios. This is explained due to a trade-off between high recovery and purity. The initial increase in CO_2 recovery decreases the overall cost since the cost is determined per CO_2 captured. From a certain point, the inflection point, the increase in recovery is less significant than the energy consumption required for this effect. Since there is a direct relationship between membrane area and specific cost; eventually, the cost of increasing the membrane area to achieve higher recoveries outweighs the benefits of improved recovery, increasing the overall specific cost.

These trade-offs are presented in **Figure 15**, which directly plots the influence of recovery and purity. In **Figure 15**, higher pressure ratios yield higher purities for the same recovery values at lower pressure ratios. This is attributed to higher ratios providing better driving forces, enabling improved separation.

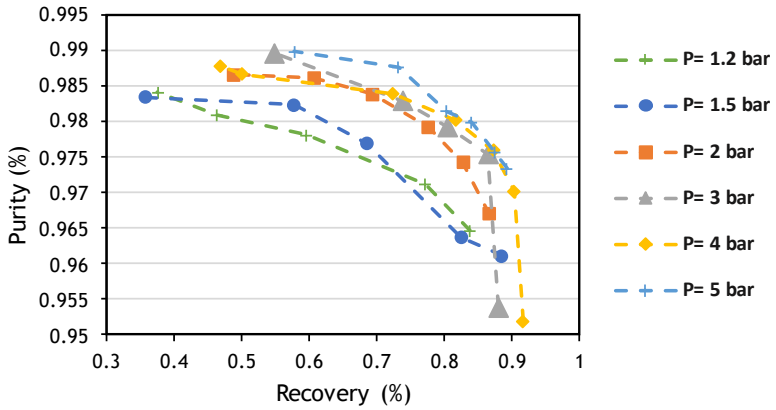

Figure 15. Recovery and Purity trade-off plot.

A decrease in CO_2 purity is observed with the increase in the process recovery. A sharp decrease is observed when the upper limit of membrane permeation is reached - total permeation condition. After analysing the membrane performance, it is important to find the optimal value of feed pressure that gives the best recovery and purity values for the lowest possible specific cost. To predict the optimal solution, **Figure 16** displays the optimal point obtained for a fixed purity of 97.5%.

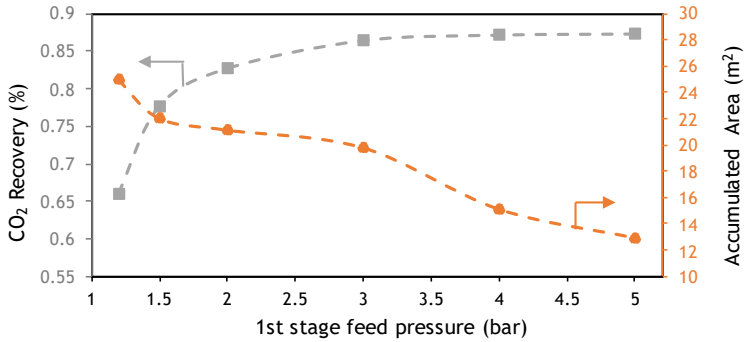

Figure 16. Relation between feed pressure, recovery, and accumulated membrane area for a fixed purity of 97.5%.

The intersection between the two curves represents the optimal operating point for membrane separation at a purity of 97.5%. The combination of feed pressure, membrane area, and recovery efficiently balances separation performance and resource utilization. In this case, using 1.4 bar as feed pressure would reach a CO_2 recovery of 77 %. As mentioned, the overall recovery percentage threshold is between 80 to 85 %. This means that the selected feed pressure will need to be slightly increased in order to respect this threshold. Therefore, for the analysed feed pressures, the best-case scenario for each was selected and compared to decide the optimized one that respects the required threshold values. **Table 11** presents the influence of feed pressure on stage 1 in the overall results.

Table 11. Operational conditions and respective separation results from a membrane separation process according to configuration A, with vacuum pressure at permeate side for all stages.

Stage 1 Feed pressure (bar)	Stage 2, 3 Feed pressure (bar)	Stage 1 area (m^2)	Stage 2 area (m^2)	Stage 3 area (m^2)	CO_2 Recovery (%)	CO_2 purity (%)	Specific Cost (€·ton^{-1})
5	1	5500	4500	2910	87.4	97.6	77.30
4		8100	4900	2100	87.2	97.5	70.80
3		12500	5000	1800	86.4	97.5	62.50
2		15000	4500	1850	82.8	97.4	51.70
1.5		28000	6500	2200	88.3	96.3	40.70
1.2		34000	6000	2000	83.7	96.3	40.80

A feed pressure of 1.5 bar is the optimal solution, reaching the lowest specific cost for this separation while respecting the defined threshold. **Figure 17** facilitates this interpretation.

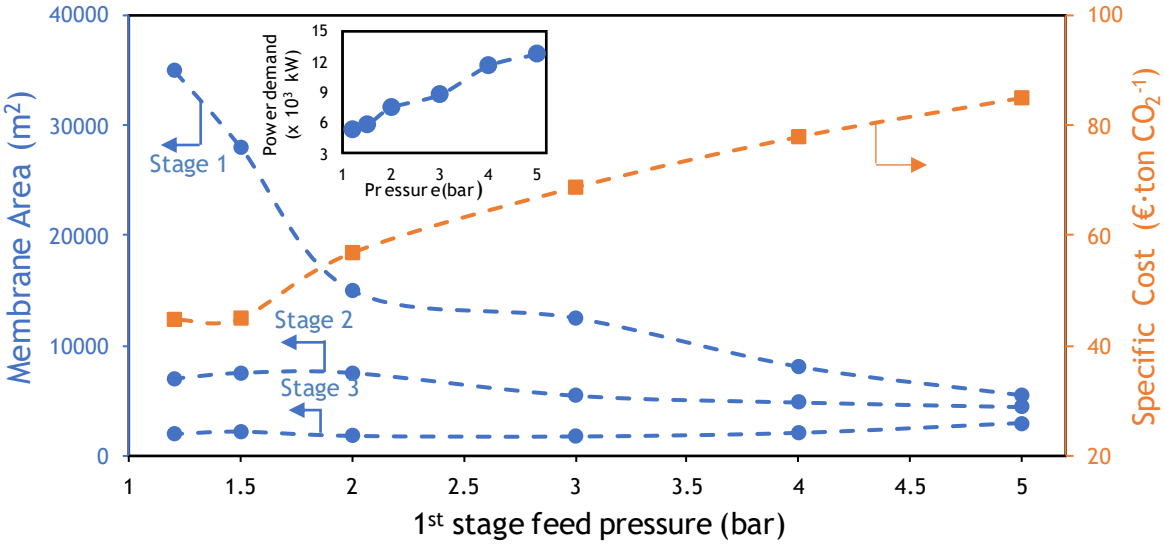

Figure 17. Schematic representation of the best configuration for the separation process using polymeric membrane technology.

Keeping the feed and permeate pressures constant for the last two stages, the membrane areas of stages 2 and 3 have a minimal influence on the cost, since they remain practically constant with increasing feed pressure of the 1st stage.

It is worth noting that the energy cost increases as the feed pressure rises. Such is due to intensified compressor energy consumption at higher pressures. When a feed pressure of 1.2 bar was applied to the 1st stage, the recovery obtained was significantly lower compared to 1.5 bar, leading to increased specific costs, moreover it requires a significant increase in the 1st stage membrane area, which also contributes to increasing the cost. Finding a key balance

between these two factors is the key to optimize energy efficiency and cost-effectiveness in the membrane separation process. The CO_2-purified gas stream leaves the process at 1 bar and ambient temperature, at 25 ºC. **Table 12** presents the overall expenditure results concerning this separation process through polymeric membrane technology for an optimised feed pressure of 1.5 bar, with **Figure 18** summarising the cost distribution for the membrane technology process.

Table 12. Overall expenditure results from a separation process with polymeric membrane technology.

	Cost values
Maintenance Cost (€·year^{-1})	1567.7
Vacuum Pumps power (kW)	4581.2
Compressor power (kW)	1266
Electricity spent (€·year^{-1})	3.74×10^6
Energy Cost (€·year^{-1})	3.75×10^6
EAC (€·year^{-1})	4.68×10^5
OPEX (€·year^{-1})	4.55×10^6
Overall Cost (€·tonCO_2^{-1})	40.70

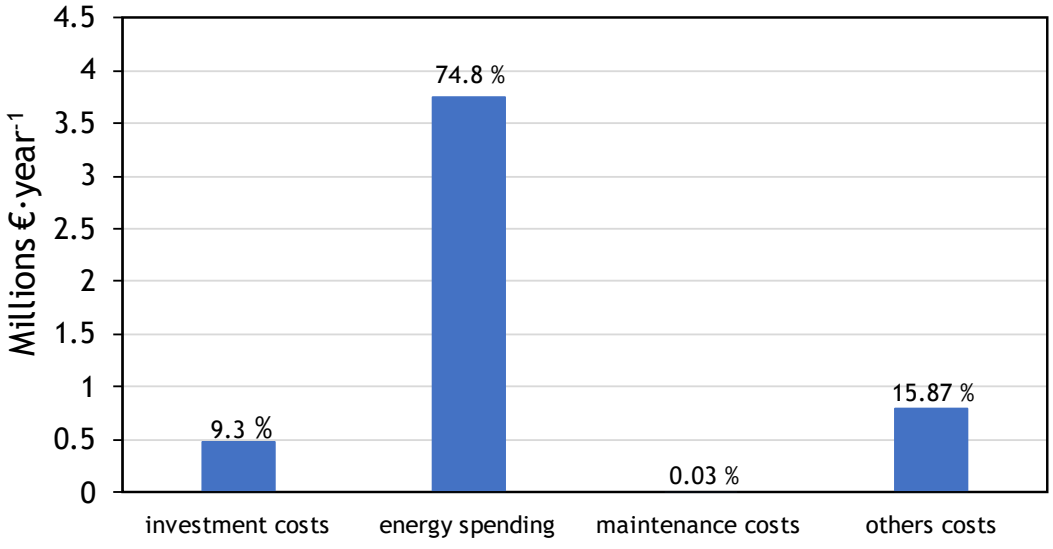

Figure 18. Cost distribution for the polymeric membrane technology process.

Once again, the energy expenditure with the utilities is the highest yearly spending. Note that, for this separation process, the only utility used was electricity, which was needed to compress the feed of stage 1, and all the three vacuum pumps used in all three stages.

4.2.3 Inorganic Membranes

As for polymeric membrane technology, its simulation was performed with the help of the developed Python-coded membrane phenomenological model. The following performance-related parameters were considered, inspired by the performance of CARBOPORA's carbon membranes for this application - **Table 13.** Permeability values are much lower than those observed with polymeric membranes, which means that a larger membrane area will be required for the separation process. A higher membrane cost will lead to higher overall costs.

Table 13. Inorganic membrane performance parameters.

	Membrane Parameters
Permeance to CO_2	91 GPU
Permeance to O_2	20 GPU
Permeance to N_2	0.5 GPU
Membrane Cost	100 €·m^{-2}

Likewise, the remaining mentioned operational parameters depend on the configuration of the membrane process itself, being necessary to define it to reach the desired results. Therefore, the first step will be determining the best configuration for the separation process.

Inorganic Membranes – Influence of overall configuration

Following the process design principles previously discussed for polymeric membranes, the number of stages employing inorganic membranes (in this case, carbon molecular sieve membranes, CMSM) was assessed to achieve the desired separation targets. Similar to polymeric membranes, up-to-three-stage scenarios were also simulated, configurated in series, for a feed pressure of 7 bar, all in the presence of vacuum at the permeate side. As presented in **Table 14**, three stages do not allow purity values above the discussed range. However, as the recovery is at 85 %, a fourth stage would not provide a significant improvement in the overall results. This way, three stages constitute the optimal solution, taking into account the associated error.

Table 14. Stage number influence on overall membrane separation performance.

Number of stages	**Feed pressure stage 1(bar)**	**Permeate pressure all cases (bar)**	**Feed pressure stage 2 (bar)**	**Feed pressure stage 3 (bar)**	**Recovery (%)**	**Purity (%)**
1	7	0.1	-	-	92.3	72.5
2	7	0.1	1	-	89.3	85.2
3	7	0.1	1	1	85.7	91.3

A 1st stage feed pressure of 7 bar was selected as the highest possible pressure due to the overall impact that a higher driving force would have on the specific separation cost. Once again, 4 configuration options were considered: one without any recycling (Configuration A - **Figure 12)**, two with recycling coming from the retentate stream of membrane module 3 (Configuration B and C – **Figure 33** and **Figure 34** in **Appendix C**), and, one with it coming from the retentate stream of membrane module 2 (Configuration D – **Figure 35** in **Appendix C**). These comparisons are presented in **Table 15.**

Table 15. Configuration influence on overall membrane separation.

Configuration	Recovery (%)	Purity (%)
A	86.8	91.4
B	86.0	91.4
C	86.5	91.5
D	85.2	91.1

As seen in **Table *15***, the presence of recycling offers almost no variation in the recovery and purity values. As a result, configuration A is selected as optimal - **Figure 12.**

Inorganic Membranes – Influence of feed pressure

The 1st stage pressure ratio was also optimized for the CCS process with inorganic membranes. The chosen pressures will determine the membrane area required for each stage to reach the threshold values for CO_2 recovery and purity. As inorganic membranes have lower permeance values (but higher selectivities), a higher range was considered, from 5 to 7 bar. Once again, to minimise the energy costs, the feed pressures for the second and third stages were kept at 1 bar, with vacuum as the permeate pressure of all three stages. The influence of the 1st stage feed pressure on the CMSM separation performance is presented in **Figure 19** and **Figure 20**.

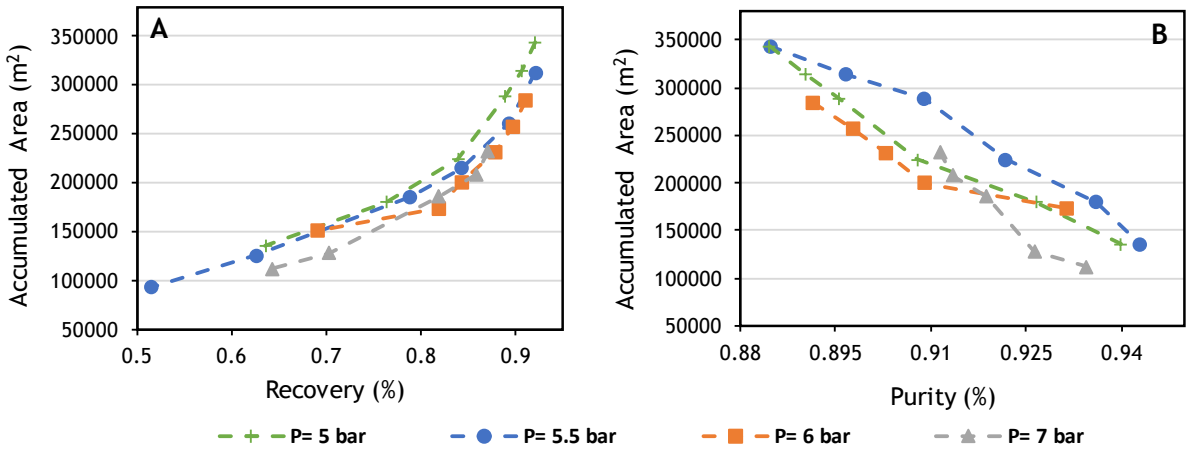

Figure 19. *A) Relation between recovery and accumulated membrane area, and B) Relation between purity and accumulated membrane area for various feed pressures with 3 inorganic membrane stages.*

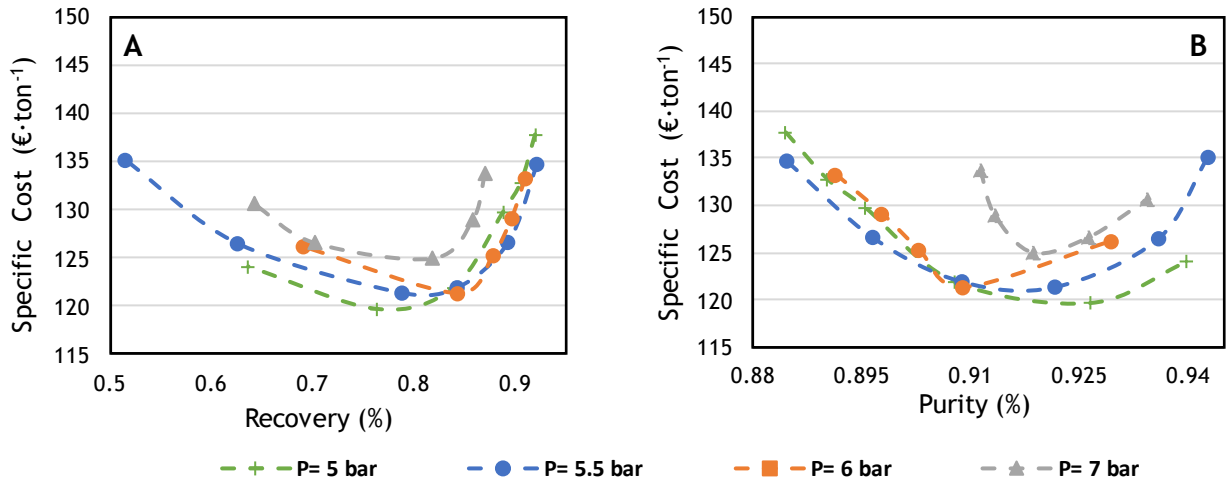

Figure 20. A) Relation between purity and specific cost, and B) Relation between purity and specific cost for various feed pressures with 3 inorganic membrane stages.

The results in **Figure 19** present a similar behaviour to those obtained for the polymeric membranes. Increasing the membrane area for the 1st stage enhances the CO_2 recovery. A larger membrane area improves separation efficiency by providing more surface area for CO_2 passage, reducing CO_2 purity. Similarly, **Figure 20** presents an inflection point for recovery and purity regarding the specific costs. These figures demonstrate a trade-off between high recovery and high purity. Lower recovery rates increase the specific cost required for high purities. After the inflection point, to reach high recoveries and purities, it is necessary to increase membrane area and spend more energy, which raises the overall system cost. Additionally, there is a trade-off between membrane area and specific cost. Once a certain threshold is surpassed, the cost associated with increasing the membrane area outweighs the benefits gained from improved recovery. A lower membrane area is needed for the simulation with a higher-pressure ratio due to the more significant driving force, as seen in **Figure 19**. Nevertheless, **Figure 20** exhibits higher specific costs for the simulation with a higher-pressure ratio due to increased energy consumption. Therefore, it is determined that energy spending is more impactful on the overall cost than membrane area. The result between recovery and purity is presented in **Figure 21.**

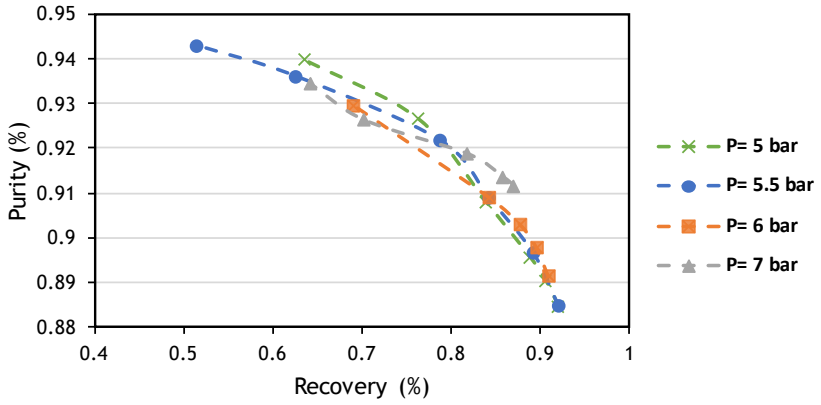

Figure 21. Recovery and Purity trade-off plot.

As mentioned, there is an overall decrease in purity with the increase in the CO_2 recovery rate. As with polymeric membrane technology, it is important to discover the optimal value of feed pressure that provides the best recovery and purity values for the lowest possible overall cost. From **Table 14** it is clear that this type of membrane will not likely allow reaching the defined thresholds, so the study will attempt to achieve the closest possible performance metrics while minimizing the overall separation costs. Therefore, for the analysed feed pressures, the best case for each was selected and compared, in order to correctly decide on the most optimal option. **Table 16** presents the influence of the feed pressure on stage 1, on the overall CO_2 recovery and purity.

Table 16. Operation conditions and results from inorganic membrane separation according to configuration A, with vacuum pressure at permeate side for all stages.

Stage 1 Feed pressure (bar)	Stage 2, 3 Feed pressure (bar)	Stage 1 area (m^2)	Stage 2 area (m^2)	Stage 3 area (m^2)	CO_2 Recovery (%)	CO_2 purity (%)	Specific Cost (€·ton^{-1})
7	1	90000	75000	45000	85.6	91.3	129.00
6		80000	63000	40000	81.9	93.1	118.80
5.5		85000	60000	45000	78.8	92.1	121.40
5		110000	69000	40000	83.9	93.8	121.90

As seen from the previous table, a feed pressure of 6 bar is the optimal condition, reaching the lowest specific cost. As discussed, the purity value is below the defined threshold of >95 %. **Figure 22** assists the reading from **Table 16**.

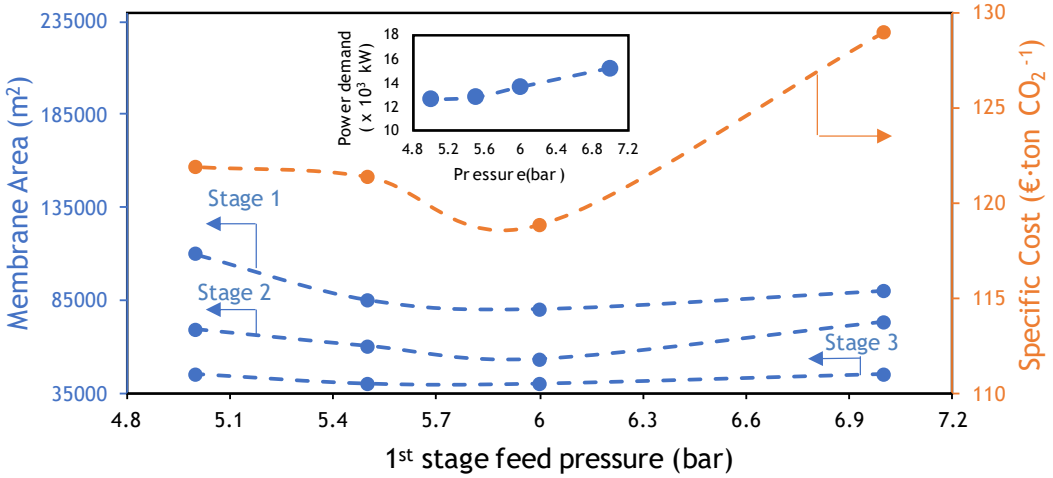

Figure 22. Schematic representation of the best configuration for the separation process using inorganic membrane technology.

The optimized feed pressure for the first membrane stage is around 5.9 to 6 bar. Likewise, in the polymeric membranes CCS process, the areas of stages 2 and 3 have minimal influence on

the cost. However, higher feed pressure results in increased energy consumption due considerably high compressor usage. For a feed pressure of 5.5 bar, although energy expenditure is lower, stage 1 requires a significant increase in membrane area, raising its cost. A lower driving force at 5.5 bar leads to a significantly lower recovery CO_2 rate compared to 6 bar, increasing the specific cost. Similarly, to other separation processes, the CO_2 gas stream exits the process at atmospheric pressure (1 bar) and ambient temperature, around 25 ºC.

Table 17 presents the economic results for this separation process employing inorganic membrane technology for an optimal feed pressure of 6 bar, also summarised in **Figure 23**.

Table 17. Overall expenditure results for a separation process with inorganic membranes.

	Cost values
Maintenance Cost (€·year^{-1})	3.91×10^5
Vacuum Pumps power (kW)	6227.3
Compressor power (kW)	6890
Electricity spent (€·year^{-1})	8.40×10^6
Energy Cost (€·year^{-1})	8.40×10^6
EAC (€·year^{-1})	3.72×10^6
OPEX (€·year^{-1})	9.78×10^6
Overall Cost (€·tonCO_2^{-1})	118.80

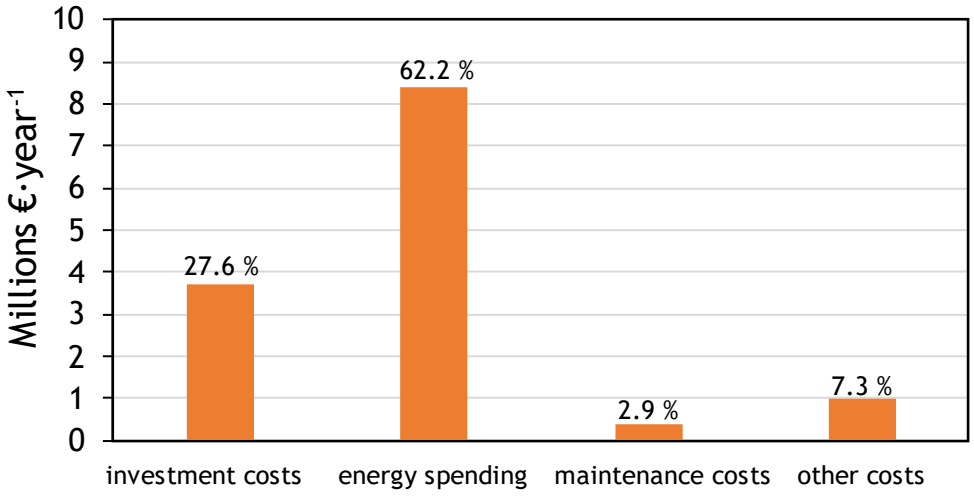

Figure 23. Cost distribution for the simulated inorganic membrane technology process.

As previously reported, the energy consumption in the process utilities is the highest yearly spending. Note that, for the separation process, the only utility used was electricity. It is also noticeable that a higher purchase value for the inorganic membranes and a higher feed pressure led to a more substantial influence of investment cost on the overall specific cost.

4.3 Purification Process

4.3.1 Purification Process post Separation by Absorption

The separation process by absorption is energy-intensive, needing a high specific cost to achieve the desired purity and recovery threshold values. This process allowed for an overall purity of 98.9 %, meaning that an additional step of purification is needed. Knowing that the main impurity of the CO_2 gas is water, a Flash separator is required to remove it, taking into account that the CO_2 stream must exit the process at 70 bar to fulfil the requirements for entry into the methanol reactor. To increase the stream purification, an additional step was added to the overall process, entirely simulated with the Aspen Plus software - **Figure 24.**

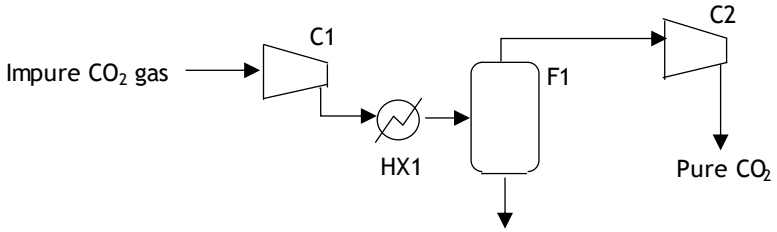

***Figure 24**. Schematic representation for the purification process after separation with Absorption.*

There is an increase in energy spending for the purification process, as a coolant is needed for the Flash separation and heat exchanger. The electricity usage will also increase, given the need of adding two new compressors in the process. **Table 18** presents the overall expenditure results concerning both the Separation and Purification processes together.

Table 18. Overall expenditure results for Separation+Purification process post Absorption separation.

	Absorption with MEA
Maintenance Cost (€·year^{-1})	2.10×10^5
Pumps power (kW)	5.17
Compressor power (kW)	1746
Steam cost (€·year^{-1})	5.73×10^6
Refrigerant cost (€·year^{-1})	1.40×10^6
Electricity cost (€·year^{-1})	1.12×10^6
Energy Cost (€·year^{-1})	1.13×10^7
EAC (€·year^{-1})	1.08×10^5
OPEX (€·year^{-1})	1.24×10^7
Overall Cost (€·tonCO_2^{-1})	111.40

The overall process obtained CO_2 at 70 bar and 30 ºC, for a recovery of 87.5 % and a purity of 99.8 %. This purity, while not 99.9 %, isk high enough considering that water is the predominant impurity, not being significant to create difficulties for the reaction to occur inside the methanol reactor. The entire process, Separation+Purification cost is 111.40 €·tonCO_2^{-1}.

4.3.2 Purification Process post Separation by Membrane Technology

The separation process with membrane technology was found to be the most cost-effective way to achieve the desired threshold values. Both separations with polymeric and inorganic membranes have purities below 99.9 %, so a purification step is needed to increase the CO_2 purity while increasing the overall CO_2 pressure to 70 bar. To this end, the purification process presented in **Figure 25** was applied to the gas stream from both processes of membrane technology. The Flash separators operate based on the conditions defined by the compressors and heat exchanger that precedes them. Compressor 3 (C_3) increases the overall CO_2 pressure to 70 bar. This process involves using 4 flash separators to separate the mixture in its respective liquid and gas phases. Flash separators are devices used to separate gas and liquid by rapidly reducing the pressure, causing the gas to separate from the liquid phase. Changing pressure and temperature before entering the Flash helps optimize the separation process by altering the phase behaviour of the mixture, enhancing the efficiency of gas-liquid separation, and facilitating the removal of impurities.

Note that every separator works at the conditions defined by the heat exchanger and compressor that precedes it. The only difference between the purification process for each membrane technology resides in the operating conditions concerning the second Flash separator; inorganic membranes need higher pressures to ensure purity values above 99.9%, as its purity after the separation process is considerably lower than that obtained with polymeric membrane technology.

The compressor that precedes the first Flash separator is a multistage compressor, with 2 stages, using refrigerant liquid as an inter-cooler. It is used to ensure that the pressure increment doesn't create a significant temperature increase. Therefore, this equipment allows a more cost-effective way to perform this pressure change while preventing the flow stream from reaching higher temperatures. Note that the gas stream leaving the second Flash separator is not reused in the process; the same does not happen with the other three Flash separators. All other gas streams leaving the top of flash separators are recycled, allowing higher CO_2 recovery for the needed purity. The decision not to recycle the gas stream from the second Flash separator was necessary to reduce the overall process costs. The overall equipment characteristics are present in the appendixes.

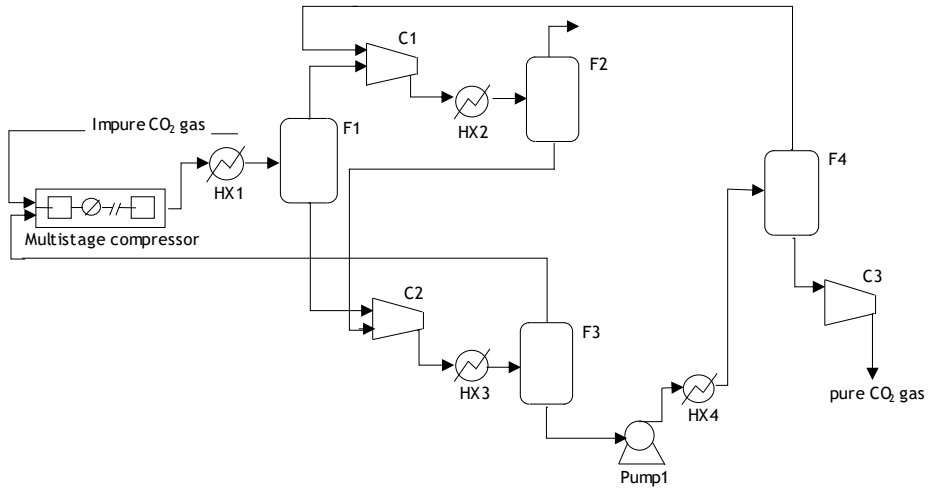

Figure 25. Schematic representation of the designed purification process for both membrane technologies – polymeric and inorganic.

The purification step was assessed for several feed pressures. With this, it is possible to evaluate the overall specific cost representing the sum of both CCS stages (separation + purification). The feed pressure influence on the specific cost and the total energy expenditure of the entire CCS process for the types of membrane technologies evaluated is presented in **Figure 26**, which includes the separation and purification stages.

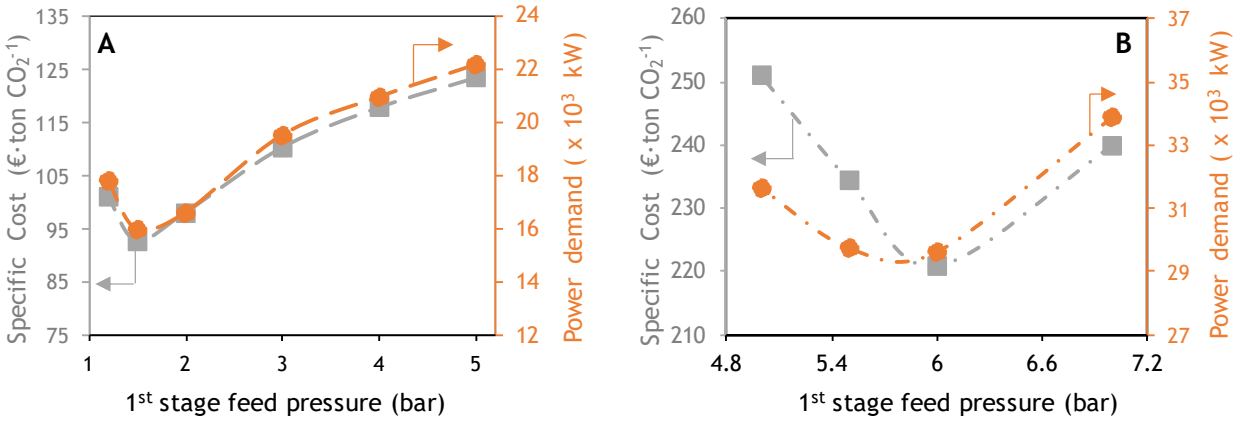

Figure 26. Feed pressure influence on the specific cost and power demand for Separation + Purification process with: A) polymeric membranes and B) inorganic membranes.

For both cases, A and B, there is an inflection point for the power demand and the specific cost. For polymeric membranes, this inflection point is at 1.5 bar, while for the inorganic membranes, is at 6 bar. These optimal feed pressure values for the first membrane stage are in accordance with what was found for the separation processes isolated. In both graphs, a higher feed pressure leads to significant energy requirements and costs due to increased power consumption. Before the inflection point, the insufficient driving force requires higher power demand to reach high purity and recovery levels, increasing the overall process costs and energy requirements. **Table 19** presents the overall expenditure results concerning this Separation and Purification processes for both membrane technologies.

Table 19. Overall expenditure results concerning this Separation+Purification processes through both membrane technologies for a feed pressure of the optimised values of 1.5 and 6 bar.

Cost values for the Separation and Purification stages combined		
	Polymeric membrane technology	**Inorganic membrane technology**
Maintenance Cost (€·year^{-1})	9.02×10^4	4.29×10^5
Pumps power (kW)	4582	6227.8
Compressor power (kW)	4666	1.22×10^4
Hot oil cost (€·year^{-1})	4.86×10^5	9.34×10^5
Refrigerant cost (€·year^{-1})	2.57×10^6	4.07×10^6
Water cost (€·year^{-1})	1.41×10^4	1.96×10^4
Electricity cost (€·year^{-1})	5.92×10^6	1.18×10^7
Energy Cost (€·year^{-1})	8.99×10^6	1.68×10^7
EAC (€·year^{-1})	7.30×10^5	4.04×10^6
OPEX (€·year^{-1})	9.90×10^6	1.83×10^7
Overall Cost (€·tonCO_2^{-1})	93.24	221.50

4.4 Technology comparison

Three separation technologies were studied in this work for CCS: absorption with MEA, polymeric membrane separation, and inorganic membrane separation. Additionally, a purification/liquefaction process was assessed through simulation for all three separation technologies to achieve the proposed thresholds in terms of purity and recovery. Recovery must be above 80 %, with purity close to 99.9 %. **Table 20** compares the most important results.

Table 20. Comparison of Performance and Cost Metrics for Simulated CCS Processes in Separation and Purification Stages combined.

Separation Process			
	CO_2 Purity (%)	CO_2 Recovery (%)	Specific cost (€·ton^{-1})
Absorption with MEA	98.9	88.9	86.83
Polymeric membranes	96.3	88.3	40.70
Inorganic membranes	93.1	81.9	118.80
Separation+Purification Processes at 70 bar			
Absorption with MEA	99.800	87.5	111.40
Polymeric membranes	99.925	82.1	93.24
Inorganic membranes	99.925	72.5	221.50

Polymeric membrane technology is the most cost-effective process to recover CO_2 from flue gas. The presented figures (**Figure 27** and **Figure 28**) compare the cost distribution of the three simulated scenarios, considering just the separation step for the first Figure and the combined steps of Separation and Purification for the second one.

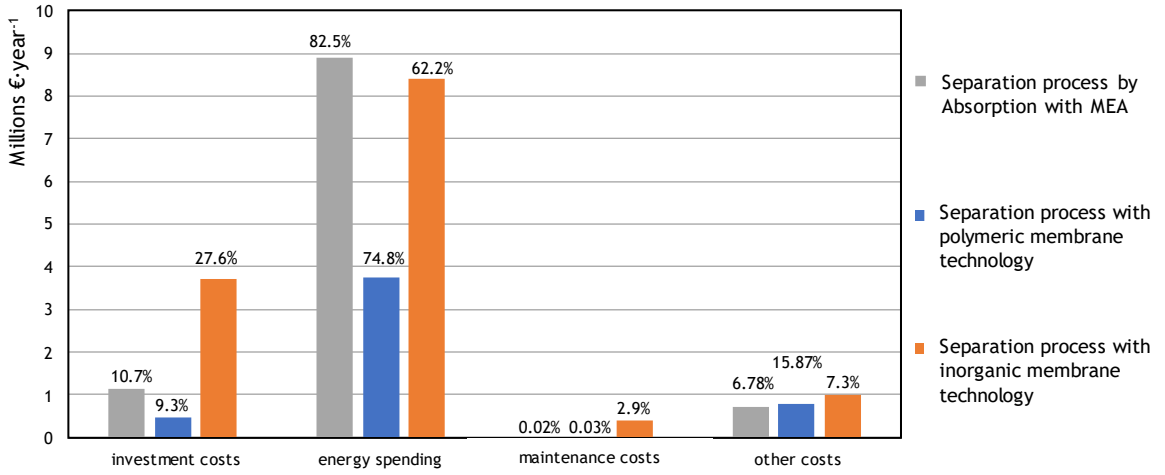

Figure 27. Entire cost distribution for all three simulated Separation processes.

As seen in **Figure 27**, the separation process by absorption is the most energy-intensive, while inorganic membranes require the highest investment due to considerable membrane costs. The membrane separation using polymeric membrane technology distances itself as the most cost-effective process regarding both parameters mentioned.

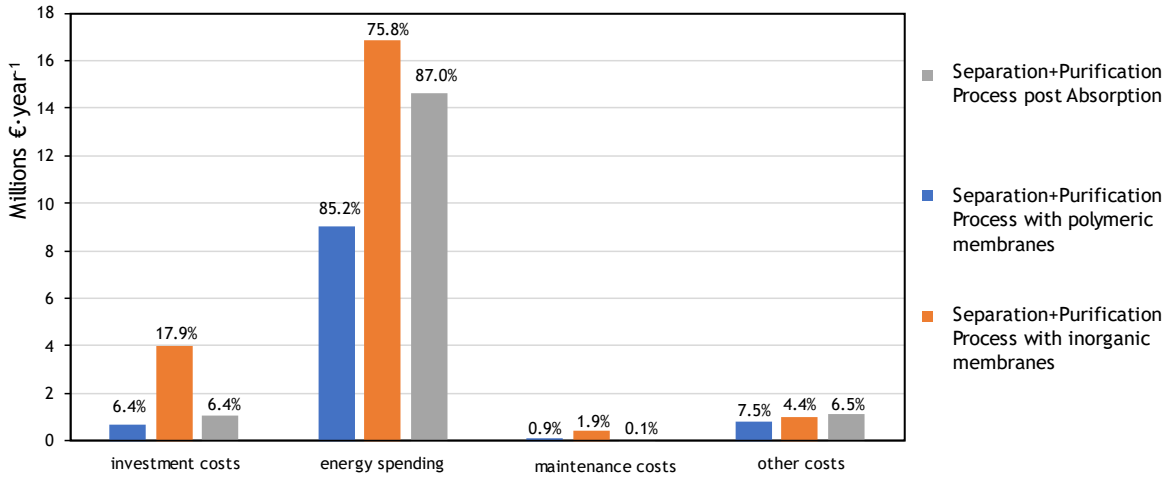

Figure 28. Cost distribution for the simulated Separation+Purification processes.

CCS process using the absorption process or inorganic membrane technology would be much more expensive, with significant energy costs associated when compared with polymeric membrane technology - **Figure 28**. Nonetheless, since this thesis also aims to optimise inorganic membrane technology from Carbopora, a sensibility analysis is performed to assess the impact of varying inputs on the overall inorganic membranes' performance.

4.5 Sensitivity Analysis

4.5.1 Influence of Electricity Cost

With the covid-19 pandemic, and the overall inflation causing substantial fluctuations in electricity costs, it becomes important to conduct a sensitivity analysis to evaluate the effect that this parameter has on the overall cost for the process with Separation and Purification combined. In this section, the cost was varied within the 0.05 to 0.2 €·kWh^{-1} to assess its influence on the overall CO_2 separation and purification cost - **Figure 29**.

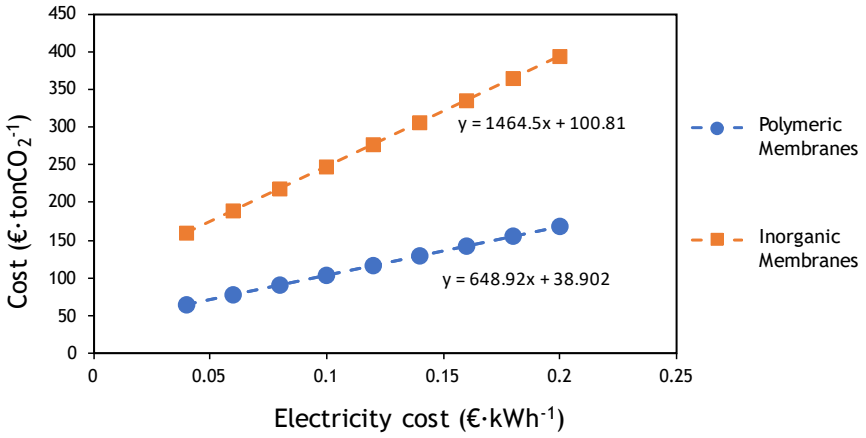

Figure 29. Influence of Electricity cost on overall cost for Separation+Purification for both polymeric and inorganic membranes.

The overall specific cost in both cases exhibits a direct and proportional relationship with the electricity cost. As the cost of electricity increases, the overall specific cost also rises linearly. It is also seen that the slope regarding inorganic membranes is more accentuated, meaning that electricity has an overall bigger effect on the specific cost. This happens due to this technology needing higher driving forces for the separation, therefore increasing the power demand at the compressors and pumps.

4.5.2 Influence of Inorganic Membrane Cost

Most inorganic membranes reported in the literature, as is the case with Carbopora, remain at the small scale, therefore being important to understand how their overall production cost will influence the specific cost of real separation and purification processes based on this technology. With it being a newer technology, purchase prices are more likely to fluctuate. The inorganic CMSM membrane cost variation was set from 25 to 200 €·m^{-2}, and its influence on overall process cost is found in **Figure 30.** The specific process cost increased linearly with the membrane purchase price, meaning that a lower acquisition value for inorganic membranes will lead to an overall lower expenditure.

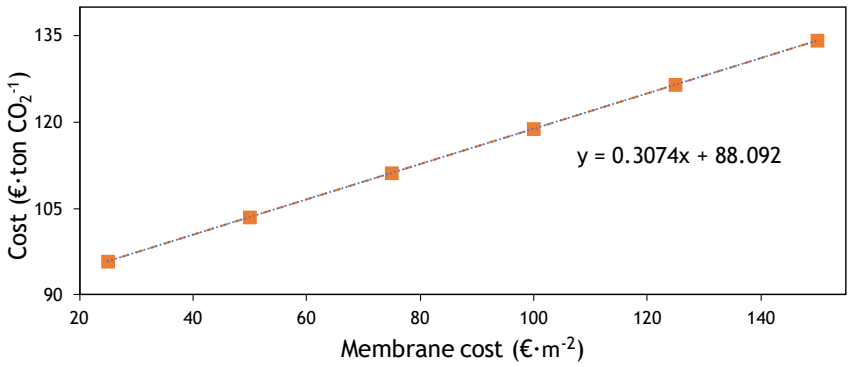

Figure 30. Influence of membrane cost on specific cost of Separation+Purification for inorganic membrane technology.

4.5.3 Influence of Inorganic Membrane Permeances

Membrane selectivity is the ratio between respective permeance values for each gas. From **Table 13**, the CO_2/O_2 selectivity is 4.55 and CO_2/N_2 selectivity is 182. Since Carbopora's inorganic membranes have a lower CO_2 permeability than polymeric membranes, this parameter will be studied. The aim is for Carbopora to become competitive in the membrane separation market. Based on the information provided by the company, the CO_2 permeance of the membranes has the potential to increase to 1000 GPU. Its influence was studied while keeping the O_2 and N_2 permeance values constant - **Figure 31.**

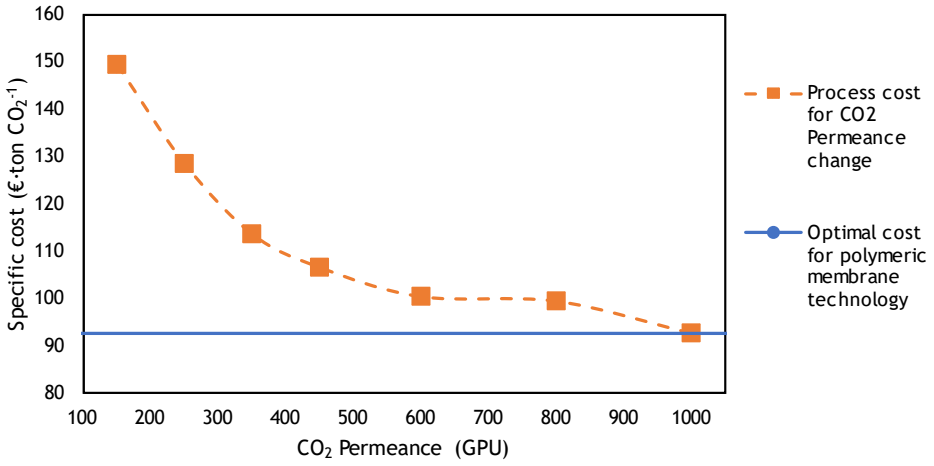

Figure 31. Influence of the CO_2 permeance on overall specific cost of Separation+Purification for inorganic membrane technology compared with the optimal cost for polymeric membrane technology.

Maintaining permeances for O_2 and N_2 constant, the permeance for CO_2 would need to increase to its highest evaluated value of 1000 GPU to compete with polymeric membrane technology. Accordingly, both processes would require an overall specific cost of around 93.00 €·ton CO_2^{-1}, to obtain a purified and liquid CO_2 at 70 bar, with purity above 99.9 % and recovery of at least 80 %. This way, permeances would need to be 1000 GPU, 20 GPU, and 0.5 GPU for CO_2, O_2, and N_2 permeances, respectively. This is an overall increase of selectivity by a factor of around 11.

5. Conclusion

In conclusion, this work focused on developing and optimizing industrial-scale processes for separating and purifying CO_2 from a stationary point source, the biomass co-generation power plant from Capwatt at Sonae. The study aimed to survey several carbon capture and storage (CCS) technologies to identify the most suitable option. The selected technologies for evaluation included membrane separation, polymeric and inorganic, and MEA absorption. A simulation software, Aspen Plus, was used to simulate separation and purification processes. In addition, an innovative Python model was developed to simulate membrane separation performance to better predict the techno-economic feasibility of using it to perform CCS.

The results obtained from the separation process using MEA solvent showed non-competitive results. The overall cost of this process was found to be in line with similar processes reported in the literature at 86.83 €·tonCO_2^{-1}, with high purity at 98.9 %. The energy consumption associated with utilities emerged as the major contributor to the overall cost. For the membrane separation technology, the developed model was validated and compared with simulators reported in the literature. The optimization of membrane area and feed pressure are of utmost importance because their optimization allows obtaining the desired CO_2 recovery and purity values. The analysis revealed a trade-off between membrane area and specific cost. The optimal configuration for the polymeric membrane technology process was with 3 stages and a feed pressure of 1.5 bar, yielding the lowest specific cost for CO_2 separation at 40.70 €·tonCO_2^{-1}. Similarly, the inorganic membrane technology process was optimized, and a feed pressure of 6 bar was determined to be the optimal value. The cost distribution analysis highlighted the influence of the energy spending due to increased feed pressure on the overall specific cost, reaching 118.80 €·tonCO_2^{-1}. For all separation technologies, the CO_2 purities obtained were below 99.9 %. To increase CO_2 purity and pressure for further use in the hydrogenation reactor, two purification processes were designed. Flash separators were employed to change the pressure while maintaining a high CO_2 recovery. The purification process following Absorption was simpler when compared with the process following membrane separation. The overall added cost for separation and purification is 111.40 €·tonCO_2^{-1}, 93.24 €·tonCO_2^{-1}, and 221.50 €·tonCO_2-^{1} for Absorption, polymeric, and inorganic membrane technology, respectively. Carbopora's inorganic membranes, due to high specific cost, need an increase in CO_2 permeance to 1000 GPU, to reach 93.00 €·tonCO_2^{-1}, becoming competitive.

In conclusion, this master thesis work has successfully developed and optimized novel processes for renewable energy production, with polymeric membrane technology being the most promising one. The results obtained show the feasibility and cost-effectiveness of membranes, paving the way for their practical, clean, and cost-effective implementation for CCS.

6. Assessment of the work done

6.1 Future Work

Increasing CO_2 purity is the most energy-intensive and expensive process step, as the flue gas stream only contains 14.5 % of CO_2. Therefore, future work should focus on increasing this concentration before the separation process. The solution may involve performing oxycombustion. Oxycombustion relates to burning the fuel with pure oxygen instead of air, resulting in a flue gas comprising water vapor (H_2O) and carbon dioxide (CO_2). By eliminating nitrogen from combustion, the flue gas can contain up to 90 % of CO_2, making its capture and storage easier and more cost-effective. Another possible strategy to achieve higher CO_2 purities at a lower cost would be by mixing the two membrane technologies in one single process, taking advantage of their strengths. This idea was briefly simulated, as described in the next section.

6.2 Other Work Carried Out

The combination of both membrane technologies was briefly simulated as a potential future work development. These preliminary studies indicated that three membrane stages were the optimal scenario to achieve purities for CO_2 above 99.9 %. The first two stages considered polymeric membranes, while the third stage comprised inorganic membranes from Carbopora with the same parameters presented in **Table 12.** This process allowed recycling, as observed in configuration B on Appendix C, which allows for higher CO_2 purity and recovery without significantly increasing the specific cost. This combined process proved to be less expensive than MEA absorption and separation with inorganic membranes, costing around 65 €·tonCO_2^{-1} for the separation process. At this stage, the overall costs of this combined process are still higher than the polymeric membrane technology, but it provides a clear recommendation of the urgent need for Carbopora to focus on developing inorganic membranes with improved CO_2 permeances. In this case, an increase in CO_2 permeance to 450 GPU would be enough for Carbopora to be involved in a competitive solution. Such means that the permeance increase to 1000 GPU as predicted, would make this solution as the most competitive in the CCS market.

6.3 Final Assessment

The work developed this semester allowed me a much deeper understanding of the need for energy transition. I developed clear knowledge of carbon separation technologies and their overall impact on the environmental crisis. Therefore, I am now in the privileged position of being a part of a program that has the opportunity of changing the climate and help prevent what can be described as one of the greatest threats of the 21st century.

7. References

[1] K. O. Yoro and M. O. Daramola, "CO_2 emission sources, greenhouse gases, and the global warming effect," in *Advances in Carbon Capture: Methods, Technologies and Applications*, Elsevier, 2020, pp. 3–28. doi: 10.1016/B978-0-12-819657-1.00001-3.

[2] I. Energy Agency, "Global Energy Review: CO_2 Emissions in 2021 Global emissions rebound sharply to highest ever level," 2021. [Online]. Available: www.iea.org/t&c/

[3] B. Filipa da Silva Soares, I. Maria Marrucho Fausto Gallucci, H. Matos Supervisor, and I. Maria Marrucho, "CO_2 Separation using Carbon Molecular Sieving and Mixed-Matrix Membranes Chemical Engineering Examination Committee," 2020.

[4] V. Gupta, A. Paula Vieira Soares Pereira Dias in, K. Sztekler, E. Caetano Fernandes Supervisor, and A. Paula Vieira Soares Pereira Dias, "Modelling of CO_2 capture using Aspen Plus for EDF power plant, Krakow, Poland Energy Engineering and Management Examination Committee," 2016.

[5] Sonae Capital, "SIAF Green Bond | Impact Report," Apr. 2021.

[6] S. Kanuri, S. Roy, C. Chakraborty, S. P. Datta, S. A. Singh, and S. Dinda, "An insight of CO_2 hydrogenation to methanol synthesis: Thermodynamics, catalysts, operating parameters, and reaction mechanism," *International Journal of Energy Research*, vol. 46, no. 5. John Wiley and Sons Ltd, pp. 5503–5522, Apr. 01, 2022. doi: 10.1002/er.7562.

[7] L. L. Baxter, S. Burt, L. Baxter, and A. Baxter, "Cryogenic CO_2 Capture as a Cost-Effective CO_2 Capture Process Biomass Combustion View project Fischer-Tropsch View project Cryogenic CO_2 Capture as a Cost-Effective CO_2 Capture Process," 2009. [Online]. Available: https://www.researchgate.net/publication/264875049

[8] S. Sen, "An overview of clean coal technologies I: Pre-combustion and post-combustion emission control," *Energy Sources, Part B: Economics, Planning and Policy*, vol. 5, no. 3, pp. 261–271, Jul. 2010, doi: 10.1080/15567240903567639.

[9] M. Trupp, J. Frontczak, and J. Torkington., "The gorgon CO_2 injection project - 2012 update," in *Energy Procedia*, Elsevier Ltd, 2013, pp. 6237–6247. doi: 10.1016/j.egypro.2013.06.552.

[10] L. Strömberg *et al.*, "Update on Vattenfall's 30 MWth oxyfuel pilot plant in Schwarze Pumpe," in *Energy Procedia*, Feb. 2009, pp. 581–589. doi: 10.1016/j.egypro.2009.01.077.

[11] H. C. Mantripragada, H. Zhai, and E. S. Rubin, "Boundary Dam or Petra Nova – Which is a better model for CCS energy supply?," *International Journal of Greenhouse Gas Control*, vol. 82, pp. 59–68, Mar. 2019, doi: 10.1016/j.ijggc.2019.01.004.

[12] N. S. Sifat and Y. Haseli, "A critical review of CO_2 capture technologies and prospects for clean power generation," *Energies*, vol. 12, no. 21. MDPI AG, 2019. doi: 10.3390/en12214143.

[13] R.K. Nilavuckkarasi;, P. Muthumari;, B. Ambedkar*;, and M. Moniha, "Carbon-rich solvent regeneration in solvent-based post-combustion CO_2 capture process (PCCC): Process intensification by megasonics," *Chemical Engineering & Processing: Process Intensification*, 2020, doi: https://doi.org/10.1016/j.cep.2020.107913.

[14] B. Lv, B. Guo, Z. Zhou, and G. Jing, "Mechanisms of CO_2 Capture into Monoethanolamine Solution with Different CO_2 Loading during the Absorption/Desorption Processes," *Environ Sci Technol*, vol. 49, no. 17, pp. 10728–10735, Sep. 2015, doi: 10.1021/acs.est.5b02356.

[15] M. Ramdin, T. W. de Loos, and T. J. H. Vlugt, "State-of-the-Art of CO_2 Capture with Ionic Liquids," *Ind Eng Chem Res*, vol. 51, no. 24, pp. 8149–8177, Jun. 2012, doi: 10.1021/ie3003705.

[16] Y. Wu, J. Xu, K. Mumford, G. W. Stevens, W. Fei, and Y. Wang, "Recent advances in carbon dioxide capture and utilization with amines and ionic liquids," *Green Chemical Engineering*, vol. 1, no. 1, pp. 16–32, Sep. 2020, doi: 10.1016/j.gce.2020.09.005.

[17] A. José Rolo de Andrade, "Design and Operation Optimisation of a MEA-Based CO_2 Capture Unit Chemical Engineering Examination Committee," Instituto Superior Técnico, 2014.

[18] F. Shakerian, K. H. Kim, J. E. Szulejko, and J. W. Park, "A comparative review between amines and ammonia as sorptive media for post-combustion CO_2 capture," *Applied Energy*, vol. 148. Elsevier Ltd, pp. 10–22, Jun. 05, 2015. doi: 10.1016/j.apenergy.2015.03.026.

[19] D. Wawrzyńczak, I. Majchrzak-Kucęba, C. Pevida, G. Bonura, R. Nogueira, and M. de Falco, *The Carbon Chain in Carbon Dioxide Industrial Utilization Technologies*, First edition. 2022. doi: 10.1201/9781003336587.

[20] J. R. Alcántara-Avila, F. I. Gómez-Castro, J. Gabriel Segovia-Hernández, K.-I. Sotowa, and T. Horikawa, "Energy Minimization in Cryogenic Distillation Columns Through Intermediate Side Heat Exchangers," 2014.

[21] T. Araújo, "High-performance carbon molecular sieve membranes with highly-controlled pore size distribution," Faculty of Engineering University of Porto, 2022.

[22] B. Ladewig and M. N. Z. Al-Shaeli, "Fundamentals of Membrane Processes," 2017, pp. 13–37. doi: 10.1007/978-981-10-2014-8_2.

[23] E. Favre, "Membrane Separation Processes and Post-Combustion Carbon Capture: State of the Art and Prospects," *Membranes (Basel)*, vol. 12, no. 9, Sep. 2022, doi: 10.3390/membranes12090884.

[24] O. Agboola, O. Sunday Isaac Fayomi, R. Sadiku, P. Popoola, P. Adeniyi Alaba, and A. T. Adegbola, "Polymers blends for the improvement of nanofiltration membranes in wastewater treatment: A short review," in *Materials Today: Proceedings*, Elsevier Ltd, 2020, pp. 3365–3368. doi: 10.1016/j.matpr.2020.05.387.

[25] M. J and F. M, "CO_2 Separation from Flue Gases Using Different Types of Membranes," *J Membr Sci Technol*, vol. 6, no. 2, 2016, doi: 10.4172/2155-9589.1000153.

[26] A. K. Fard *et al.*, "Inorganic membranes: Preparation and application for water treatment and desalination," *Materials*, vol. 11, no. 1. MDPI AG, Jan. 05, 2018. doi: 10.3390/ma11010074.

[27] Y. Deng, Y. Wu, G. Chen, X. Zheng, M. Dai, and C. Peng, "Metal-organic framework membranes: Recent development in the synthesis strategies and their application in oil-water separation," *Chemical Engineering Journal*, vol. 405. Elsevier B.V., Feb. 01, 2021. doi: 10.1016/j.cej.2020.127004.

[28] A. Baldwin, S. Austin, and P. Waskett, "Capturing CO_2: Gas Compression vs. Liquefaction," *POWER*, Jun. 01, 2009.

[29] Air Liquid, "Innovation delivered for a sustainable world," 2022. Accessed: Mar. 13, 2023. [Online]. Available: https://engineering.airliquide.com/sites/engineering/files/2022-09/brochurecryocapsept2022_1.pdf

[30] T. Suda, M. Fujii, and K. Yoshida, "Development of Flue Gas Carbon Dioxide Recovery Technology," 1992.

[31] D. Kearns, "NOUMAN MIRZA, Ph.D Consultant-CCS Technologies State of the Art: CCS Technologies 2022."

[32] C. Zhang, "Absorption principle and techno-economic analysis of CO_2 absorption technologies: A review," in *IOP Conference Series: Earth and Environmental Science*, IOP Publishing Ltd, Feb. 2021. doi: 10.1088/1755-1315/657/1/012045.

[33] C. Chao, Y. Deng, R. Dewil, J. Baeyens, and X. Fan, "Post-combustion carbon capture," *Renewable and Sustainable Energy Reviews*, vol. 138, Mar. 2021, doi: 10.1016/j.rser.2020.110490.

[34] A. S. Akdag, I. Durán, G. Gullu, and C. Pevida, "Performance of TSA and VSA post-combustion CO_2 capture processes with a biomass waste-based adsorbent," *J Environ Chem Eng*, vol. 10, no. 6, Dec. 2022, doi: 10.1016/j.jece.2022.108759.

[35] J. J. Carberry *et al.*, *Plant Design and Economics for Chemical Engineers*, 4th ed. McGraw Hill, International Editions, 1991.

[36] J. Yang, J. Zhao, F. Wen, and Z. Y. Dong, "A Framework of Customizing Electricity Retail Prices," *IEEE Transactions on Power Systems*, vol. 33, no. 3, pp. 2415–2428, May 2018, doi: 10.1109/TPWRS.2017.2751043.

[37] Trading Economics, "EU Natural Gas," *Trading Economics*. https://tradingeconomics.com/commodity/eu-natural-gas?ref=vc.ru (accessed Jun. 20, 2023).

[38] Engineering ToolBox, "Fuels - Higher and Lower Calorific Values," *Engineering ToolBox*. https://www.engineeringtoolbox.com/fuels-higher-calorific-values-d_169.html (accessed Jun. 20, 2023).

[39] J. Nyári, "Techno-economic feasibility study of a methanol plant using carbon dioxide and hydrogen."

[40] W. L. Luyben, "Estimating refrigeration costs at cryogenic temperatures," *Comput Chem Eng*, vol. 103, pp. 144–150, 2017, doi: 10.1016/j.compchemeng.2017.03.013.

[41] Y. Chu, A. Lindbråthen, L. Lei, X. He, and M. Hillestad, "Mathematical modeling and process parametric study of CO_2 removal from natural gas by hollow fiber membranes," *Chemical Engineering Research and Design*, vol. 148, pp. 45–55, Aug. 2019, doi: 10.1016/j.cherd.2019.05.054.

[42] X. He, D. Chen, Z. Liang, and F. Yang, "Insight and Comparison of Energy-efficient Membrane Processes for CO_2 Capture from Flue Gases in Power Plant and Energy-intensive Industry," *Carbon Capture Science and Technology*, vol. 2, Mar. 2022, doi: 10.1016/j.ccst.2021.100020.

[43] D. Bahamon, A. Díaz-Márquez, P. Gamallo, and L. F. Vega, "Energetic evaluation of swing adsorption processes for CO_2 capture in selected MOFs and zeolites: effect of impurities."

[44] C. H. Yu, C. H. Huang, and C. S. Tan, "A review of CO_2 capture by absorption and adsorption," *Aerosol and Air Quality Research*, vol. 12, no. 5. pp. 745–769, Oct. 2012. doi: 10.4209/aaqr.2012.05.0132.

[45] T. C. Merkel, H. Lin, X. Wei, and R. Baker, "Power plant post-combustion carbon dioxide capture: An opportunity for membranes," *J Memb Sci*, vol. 359, no. 1–2, pp. 126–139, Sep. 2010, doi: 10.1016/j.memsci.2009.10.041.

Annex A - Additional information regarding equipment cost estimation

The cost of regular pumps was determined through a correlation graph that allows us to estimate the overall cost for the pumps according to their capacity. This correlation is presented in **Figure 32**.

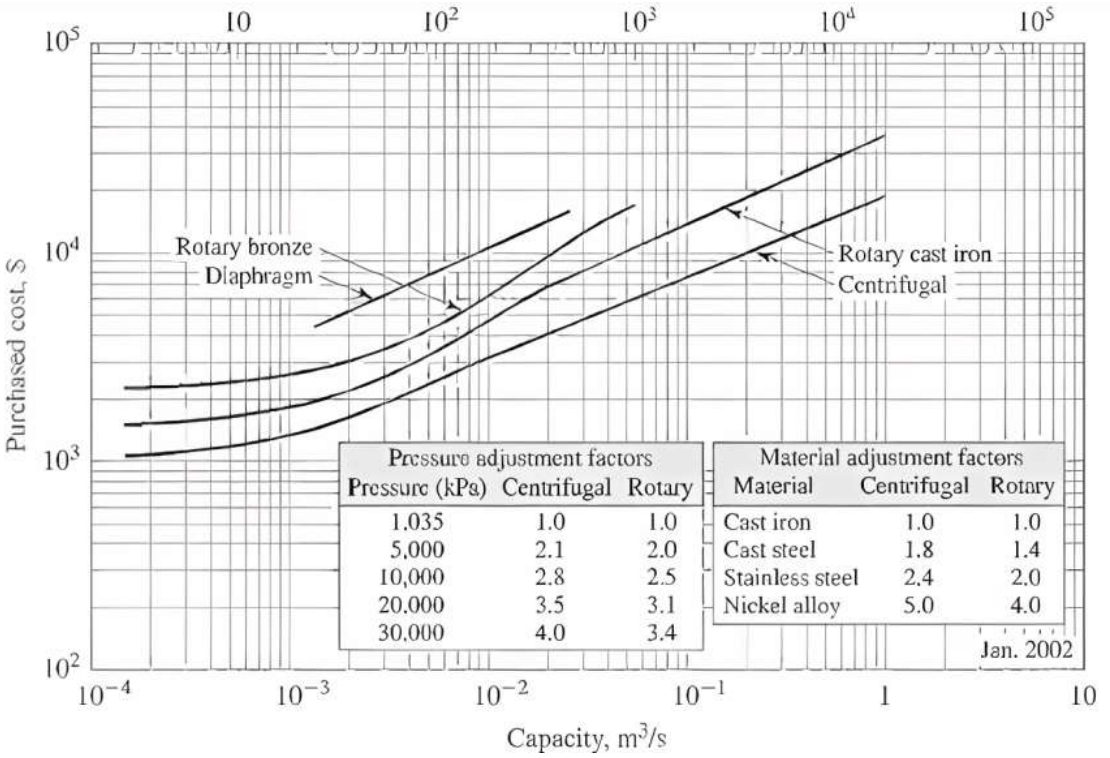

Figure 32. Pump purchase cost according to its capacity (Reproduced from [35]).

Appendix A – Additional information regarding Separation by Adsorption

Regeneration with TSA

In temperature swing adsorption, the temperature of the adsorbent is increased in order to break the bonds between the gas and the adsorbent, releasing CO_2. This process is time consuming as it needs to heat the adsorbent bed for the desorption process and requires additional time for the cooling necessary to restart the process. An alternative can be realised using adsorption by rapid electrical oscillation, solving some of the drawbacks mentioned. In this case, a low value of electric current voltage would be required to increase the temperature of the adsorbent through the Joule effect. Electrical swing adsorption (ESA) allows faster regeneration of the adsorbent but requires higher energy expenditure.

Regeneration with PSA

In PSA, the regeneration process involves lowering the adsorbent pressure to facilitate CO_2 release. High-pressure conditions cause CO_2 to adhere to the solid adsorbent surfaces, while reducing the pressure allows for its release. Once the CO_2 saturation point is reached, regeneration occurs at lower pressure levels, enabling the release of the adsorbed CO_2 and initiating a fresh cycle of CO_2 adsorption. [12].

Regeneration with VSA

VSA is a specific PSA cycle, mainly used when the feed gas is at ambient pressure, thus requiring less energy. In this process, a controlled pressure reduction is applied downstream of the feed stage to extract it at low pressure. These cycles have the potential to be used together [12].

Appendix B - Separation Processes Comparison

For the simulation component of this work, a comparison was made between the most promising separation processes to separate and store the CO_2 from the flue gas emitted by the biomass boiler.

In this regard, the performance-related metrics such as technology cost ($\$\cdot t\ CO_2^{-1}$), energy consumption ($GJ\cdot t\ CO_2^{-1}$), CO_2/N_2 selectivity and CO_2 purity (%) were critically compared. - **Table 21.**

Table 21. Decision factor for the main technologies for the separation process in CCS.

Technology	Type	Cost ($\$\cdot t\ CO_2^{-1}$)	Energy consumption ($GJ\cdot t\ CO_2^{-1}$)	CO_2/N_2 selectivity	CO_2 purity (%)	References
Absorption	MEA	40-100	3.0-4.5	-	98-99.9	[32]
	Ionic liquid	15-50	1.0-3.2	-	80-99	
	Ammonia	50-60	<3.0	-	-	
Adsorption	PSA	>80	2.8-4.2	-	>90	[33], [43], [44]
	TSA	80-150	1.0-5.0	-	>96	
	VSA	-	1.0-2.0	-	>90	
Membranes	Polymeric	20-60	-	50-200	>95	[22], [45]
	Inorganic	>60	-	>100	>98	

Appendix C - Additional configurations for Membrane Separation

Apart from the selected configuration, three other possibilities were evaluated for Membrane Separation in order to determine the most optimal configuration. These are:

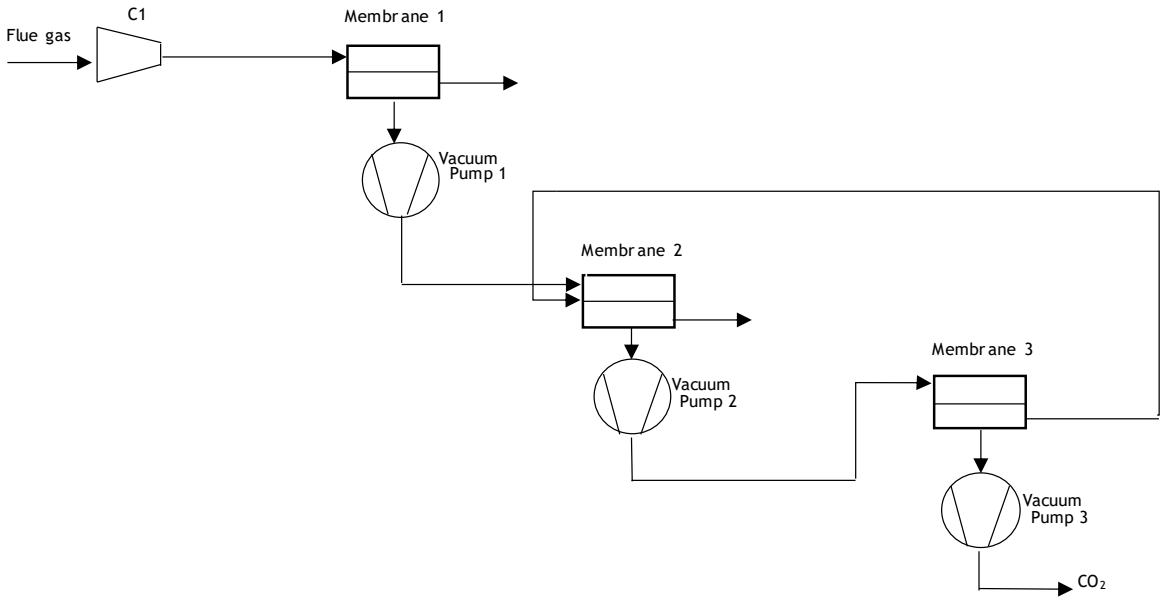

Figure 33. Schematic representation of configuration B for the Separation Process using Membrane Technology.

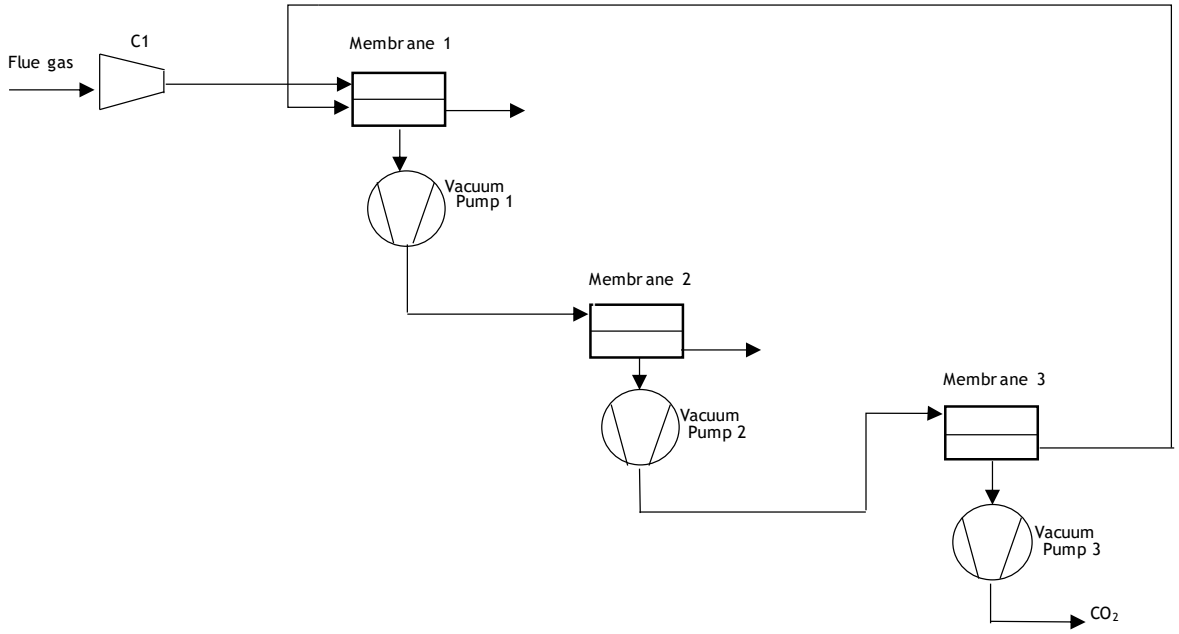

Figure 34. Schematic representation of configuration C for the Separation Process using Membrane Technology.

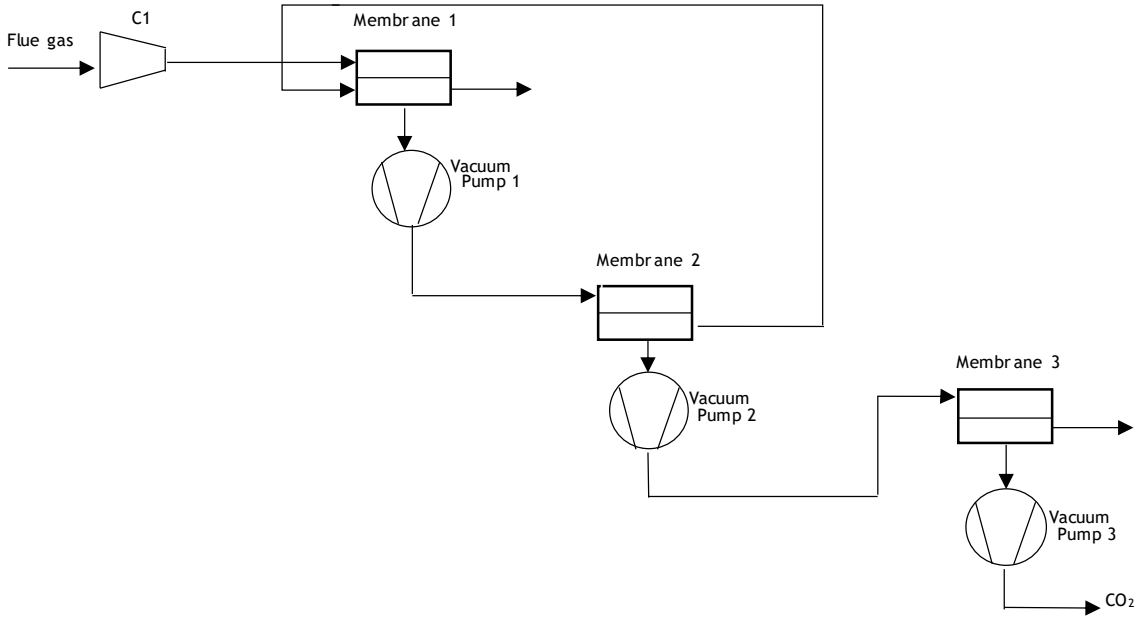

Figure 35. Schematic representation of configuration D for the Separation Process using Membrane Technology.

Appendix D – Equipment sizing for the Separation Process with Absorption

Table 22 presents the characteristics of the pumping equipment referent to the Separation Process for Absorption with MEA.

Table 22. Pumps characteristics for the Absorption Process.

	Pump1	Pump2	Pump3
Inlet Pressure (bar)	1.05	1	1.05
Outlet Pressure (bar)	1.1	1.08	1.1
Equipment type		Centrifugal	
Utility		Electricity	
Capacity ($m^3 \cdot s^{-1}$)	0.43	$5.65x10^4$	0.45

Table 23 presents the characteristics of the heat exchanger referent to the Separation Process for Absorption with MEA.

Table 23. Heat exchanger characteristics for the Absorption Process.

	Heat exchanger 1	Heat exchanger 2	Heat exchanger 3
Inlet Temperature (ºC)	73.32	103.93	97.2
Outlet Temperature (ºC)	50	103	90
Power (kW)	36290	6596.1	11775.5
Utility	Air	Steam	Air
Area (m^2)	12460	878.3	1803.3

Table 24 presents the characteristics of both columns, absorber and stripper, referent to the Separation Process for Absorption with MEA.

Table 24. Absorber and Stripper columns characteristics for the Absorption Process.

	Absorber		Stripper	
	Part1	**Part2**		
Internal Diameter (m)	4	5	5	
Weight (kg)	7791	14128	29731	
Height (m)	3	5	8.2	
Utility	-		**Reboiler**	**Condenser**
			Steam	Refrigerant liquid

Appendix E – Equipment sizing for the Separation Process with Membrane Technology

The characteristics of the individual equipment's for the Separation process with Membrane Technology, are presented in **Table 25**.

Table 25. Compressing equipment characteristics for Separation Process with Membrane Technology.

	Compressor	Vacuum Pump 1	Vacuum Pump 2	Vacuum Pump 3
Polymeric membrane technology				
Outlet Pressure (bar)	1.5	0.1	0.1	0.1
Utility	Electricity	Electricity	Electricity	Electricity
Power (kW)	1265.9	2774.2	1424.9	382.2
Inorganic membrane technology				
Outlet Pressure (bar)	6	0.1	0.1	0.1
Utility	Electricity	Electricity	Electricity	Electricity
Power (kW)	6890.0	3801.7	1243.6	1182.0

Appendix F – Equipment sizing for the Purification Process post Absorption

The characteristics of the individual compressing equipment's for the Purification Process post Absorption, are presented in **Table 26.**

Table 26. Compressing equipment characteristics for Purification Process post Absorption.

	Compressor 1	**Compressor 2**
Equipment Type	Isentropic	Isentropic
Outlet Pressure (bar)	1	45
Outlet Pressure (bar)	45	70
Utility	Electricity	Electricity
Power (kW)	1671.8	74.2

The characteristics of the individual heat exchangers for the Purification Process post Absorption, are presented in **Table 27.**

Table 27. Heat exchanger characteristics for Purification process post Absorption Process.

	Heat exchanger 1
Inlet Temperature (ºC)	4.08
Outlet Temperature (ºC)	-10
Power (kW)	36290
Utility	Refrigerant Liquid
Area (m^2)	101.8

The characteristics of the individual Flash Separators for the Purification Process post Absorption process, are presented in **Table 28.**

Table 28. Flash separators' characteristics for Purification Process post Absorption Process.

	Flash 1
Internal Diameter (m)	2
Weight (kg)	3515.5

Appendix G – Equipment sizing for the Purification Process post Membrane Separation

The characteristics of the individual compressing equipment's for the Purification Process post Membrane Technologies, are presented in **Table 29.**

Table 29. Compressing equipment characteristics for Purification Process post both Membrane Technologies Processes.

	Multistage compressor	**Comp. 1**	**Comp. 2**	**Comp. 3**	**Pump1**
Polymeric membrane technology					
Equipment Type	Isentropic	Isentropic	Isentropic	Isentropic	Centrifugal
Outlet Pressure (bar)	47	50	33	70	31.6
Utility	Electricity + Refrig. liquid	Electricity	Electricity	Electricity	Electricity
Power (kW)	3062	126.8	17.9	192.9	0.40
Inorganic membrane technology					
Equipment type	Isentropic	Isentropic	Isentropic	Isentropic	Centrifugal
Outlet Pressure (bar)	47	54	33	70	31.6
Utility	Electricity + Refrig. liquid	Electricity	Electricity	Electricity	Electricity
Power (kW)	4836	266.8	29.02	202.8	0.41

The characteristics of the individual heat exchangers for the Purification process post both membrane technologies are presented in **Table 30.**

Table 30. Heat exchangers characteristics for Purification Process post both Membrane Technologies Processes.

	Heat exchanger 1	Heat exchanger 2	Heat exchanger 3	Heat exchanger 4
Polymeric membrane technology				
Inlet Temperature (ºC)	131.2	29.2	-9.8	-4.6
Outlet Temperature (ºC)	6	-10	-4.5	-4.3
Power (kW)	2437	1151.6	1120.6	277.1
Utility	Refrigerant liquid	Refrigerant liquid	Steam	Steam
Area (m^2)	165.6	72.5	3.9	0.6
Inorganic membrane technology				
Inlet Temperature (ºC)	131.7	34.8	-12.2	-4.6
Outlet Temperature (ºC)	6	-10	-4.5	-4.3
Power (kW)	4364	2908	3317	270.8
Utility	Refrigerant liquid	Refrigerant liquid	Steam	Steam
Area (m^2)	268.8	160.3	11.2	0.6

The characteristics of the individual Flash Separators for the Purification process post both membrane technologies are presented in **Table 31**.

Table 31. Flash separators' characteristics for Purification process post both Membrane Technologies Processes.

	Flash 1	Flash 2	Flash 3	Flash 4
Polymeric membrane technology				
Internal Diameter (m)	3	6.1	3.3	1.6
Weight (kg)	8102	$3.41x10^4$	$1.01x10^4$	2216
Inorganic membrane technology				
Internal Diameter (m)	5.2	1.3	5.6	1.5
Weight (kg)	$2.44x10^4$	3648	$2.82x10^4$	4770